# Supplementary Figure 1

**a**

| GSK321 (Active Inhibitor) | | | | |
|---|---|---|---|---|
| IDH1 IC50 (nM) | | | IDH2 IC50 (nM) | |
| R132H | R132C | R132G | R140Q | R172S |
| 4.1 | 22.8 | 11.6 | 3341 | 2216 |
| **GSK990 (Inactive Inhibitor)** | | | | |
| IDH1 IC50 (nM) | | | IDH2 IC50 (nM) | |
| R132H | R132C | R132G | R140Q | R172S |
| >100,000 | >100,000 | >100,000 | >100,000 | >100,000 |

**b**

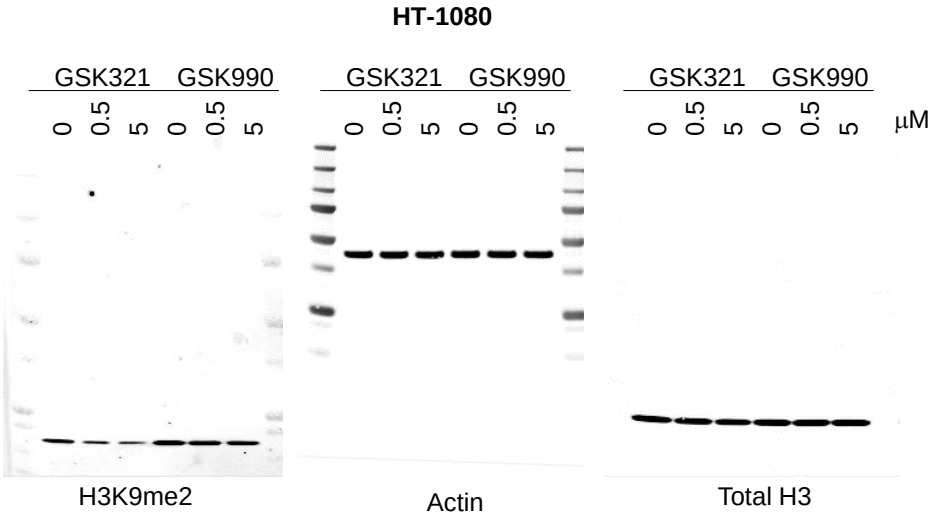


**c**

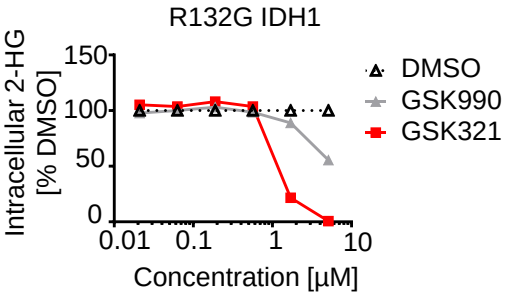


**d**

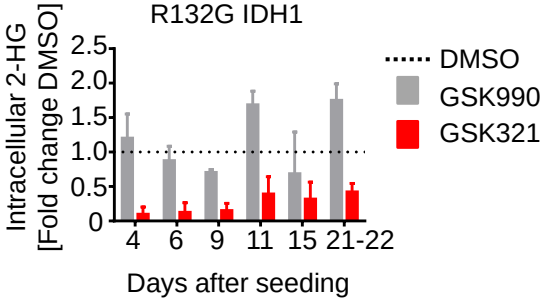

**Supplementary Figure 1. Biochemical and cellular changes induced by GSK321 allosteric inhibitor.** (**a**) Biochemical and cellular IC50 data in nM for GSK321 and GSK990 determined via NADPH oxidation. (**b**) Individual full gels showing that GSK321 leads to reduction of histone H3K9 dimethylation (H3K9me2), following treatment of R132C IDH1 expressing HT-1080 cells with increasing concentrations of GSK321 or GSK990 for 48 hours. Total H3 and Actin serve as loading control (**c**) Decreased intracellular 2-HG levels upon treatment of R132G IDH1 AML cells with increasing concentrations of GSK321. Cells were treated in suspension culture and intracellular 2-HG was measured after 7 days. 2-HG levels are normalized to total cell number and expressed relative to DMSO (%). (**d**) Treatment of primary R132G IDH1 mutant AML cells with the GSK321 inhibitor leads to a stable decrease of the levels of intracellular 2-hydroxyglutarate (2-HG) for up to 22 days in suspension culture.

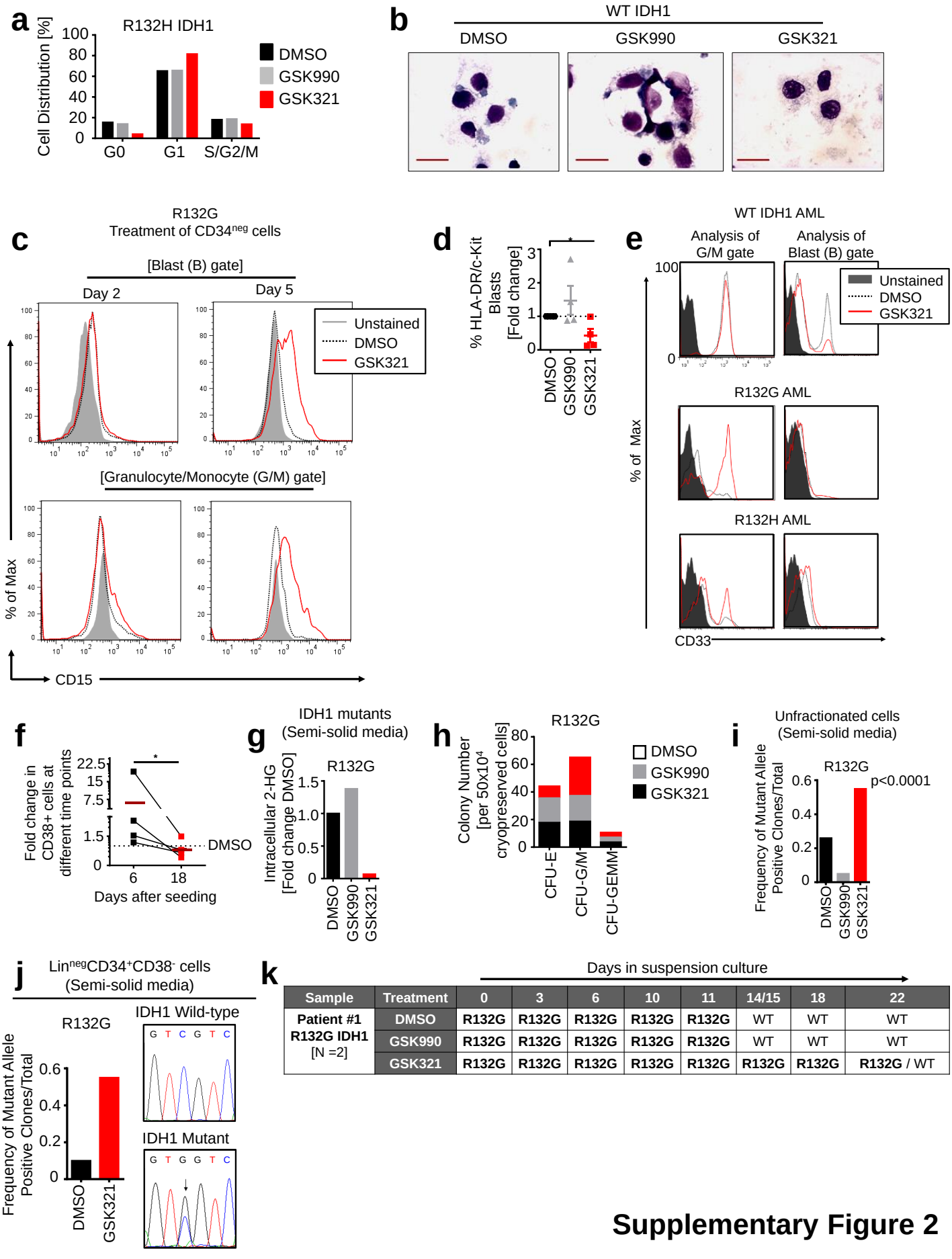


| Sample | Treatment | 0 | 3 | 6 | 10 | 11 | 14/15 | 18 | 22 |
|---|---|---|---|---|---|---|---|---|---|
| **Patient #1 R132G IDH1** [N =2] | DMSO | **R132G** | **R132G** | **R132G** | **R132G** | **R132G** | WT | WT | WT |
| | GSK990 | **R132G** | **R132G** | **R132G** | **R132G** | **R132G** | WT | WT | WT |
| | GSK321 | **R132G** | **R132G** | **R132G** | **R132G** | **R132G** | **R132G** | **R132G** | **R132G** / WT |

**Supplementary Figure 2**

**Supplementary Figure 2. Cell Biological effects of GSK321.** (**a**) Cell cycle analysis of R132H cells treated with either DMSO, GSK990 or GSK321 for 6 days in suspension culture. (**b**) Absence of morphological changes in IDH1 wild-type (WT) AML cells exposed to the GSK321 IDH1 mutant inhibitor for up to 15 days. Scale bars equals 20 μm. (**c**) Representative FACS plots evaluating CD15 expression within the Blast ($SSC^{low}$ $CD45^{low/+}$) and granulocyte/monocyte ($SSC^{high}$ $CD45^{+}$) gates. CD34neg IDH1 R132G AML cells were treated with DMSO or GSK321 for 2 days and 5 days respectively. (**d**) Frequency of HLA-DR and c-Kit double positive leukemic blasts after treatment with GSK990 or GSK321 of IDH1 mutant AML cells. Values are depicted as fold change of DMSO for 4 independent biological samples (* $p<0.05$). (**e**) Expression of the myeloid marker CD33 within the granulocyte/monocyte (G/M) and blast (B) gated cells in R132G and R132H IDH1 mutant AML cells following treatment for 6 to 7 days with DMSO, or 3 μM GSK990 or GSK321. (**f**) Analysis of CD38 expression in GSK321 treated IDH1 mutant AML cells after 6 (black) and 18 (red) days respectively. Analysis shows CD38 expression relative to DMSO treatment (dotted line). The maroon colored line represents the mean levels in each analysis (N = 4 independent biological samples). (**g**) Decreased intracellular 2-HG following single dose treatment of R132G IDH1 AML cells in semi-solid methylcellulose media supplemented with DMSO, or 3 μM GSK990 or GSK321 for 14 days. 2-HG levels are normalized to total cell numbers and represented relative to DMSO treated cells as a fold change. (**h**) Increased frequency of granulocytic/monocytic (G/M) colony forming units (CFU) in GSK321 treated R132G IDH1 mutant AML cells following treatment and growth in methylcellulose. (CFU-E, colony forming units- erythrocyte; CFU-GEMM, colony forming units-granulocyte erythrocyte monocyte macrophage). (**i**) Increased frequency of IDH1 mutant allele positive clones following treatment with the GSK321 inhibitor in semi-solid media for 10-14 days. Bar plots illustrating the frequency of IDH1 mutant allele-positive colonies as a ratio to the total number of colonies (Mutant/Total) per treatment. p-values are determined by Chi-square test. [p-value < 0.0001]. (**j**) Enrichment for cells carrying the IDH1 mutant allele following treatment of FACS fractionated lineage-negative CD34-positive CD38-negative ($Lin^{neg}CD34^{+}CD38^{-}$) cells with the GSK321 inhibitor in differentiation inducing suspension culture. Representative chromatographs of IDH WT and mutant cells are shown. (**k**) GSK321 induces differentiation of IDH1 mutant allele positive cells. Persistence of unfractionated IDH1 R132G mutant AML cells treated with GSK321 for up to 22 days in suspension cultures. Data shown represents 2 independent experiments.

**a**

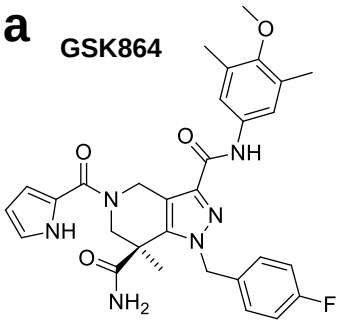


**b**

| GSK864 | | | | |
|---|---|---|---|---|
| IDH1 $IC_{50}$ (nM) | | | | |
| R132H | R132C | R132G | WT | HT1080 cell 2-HG |
| 15.2 | 8.8 | 16.6 | 466.5 | 320 |
| IDH2 $IC_{50}$ (nM) | | | | |
| R140Q | R172S | WT | R172 U87MG | SW1353 cell 2-HG |
| 1916 | 997 | 1360 | ND | 8236 |

**c**

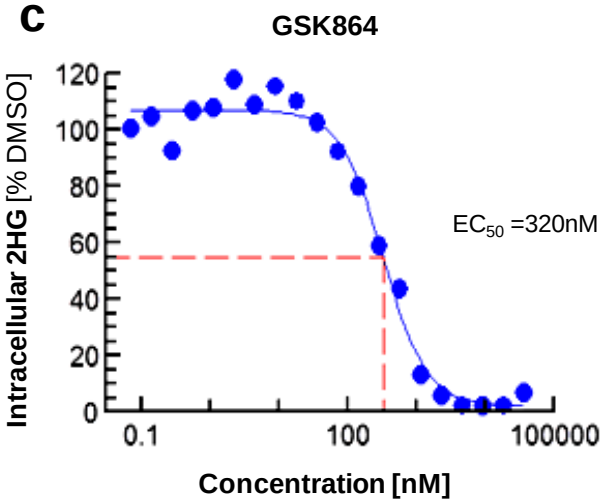


**d**

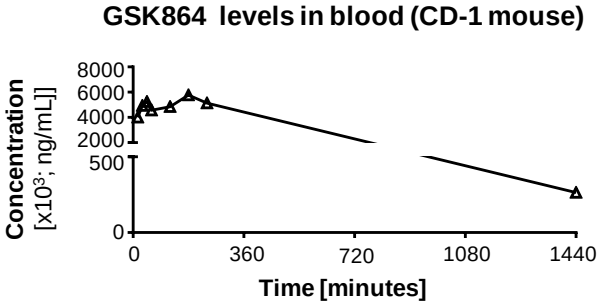


**e**

| GSK864 PK | |
|---|---|
| Intraperitoneal (IP) administration | |
| **Dose** [mg/kg] | 213 |
| **$C_{max}$** [ng/mL] | 5830 |
| **$AUC_{0-t}$** [hr*ng/mL] | 52300 |
| **$DNAUC_{0-t}$** [hr*ng/mL/mg/kg] | 246 |

**f**

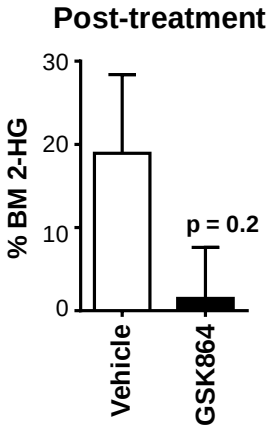


**Supplementary Figure 3**

**Supplementary Figure 3. Properties of the bioavailable GSK864 and bone marrow (BM) engraftment of IDH1 mutant AML cells.** (**a**) Chemical structure of the bioavailable GSK864 compound, an IDH1 inhibitor with improved *in vivo* pharmacokinetic properties compared to GSK321. Absolute stereochemistry for GSK864 is tentatively assigned based on *ab initio* Vibrational Circular Dichroism (VCD) analysis of intermediate *(S)*-5-*tert*-butyl 3,7-diethyl 7-methyl-6,7-dihydro-1*H*-pyrazolo[4,3-*c*]pyridine-3,5,7(4*H*)-tricarboxylate used to prepare GSK864. (**b**) Biochemical and cellular $IC_{50}$ data for GSK864. [ND, Not determined due to lack of biochemical inhibition]. (**c**) GSK864 is a potent inhibitor of IDH1-mutant enzyme and blocks production of intracellular 2-HG in IDH1 R132C mutant HT-1080 cells. The graph is a representation of two independent experiments. (**d**) Graph depicts blood concentrations of GSK864 in CD-1 mouse upon intraperitoneal (IP) injection for up to 1440 minutes. (**e**) Pharmacokinetics (PK) parameters in the CD-1 mouse following intraperitoneal (IP) administration of GSK864. Mean parameter values for up to 2 mice are displayed. (**f**) BM 2-HG (in %) levels per mice before and treatment with either vehicle or GSK864. Levels depicted as mean ± S.E.M. Data shown represents 2 mice in vehicle treatment group and 3 mice in GSK864 treatment group. [n.s., not significant].

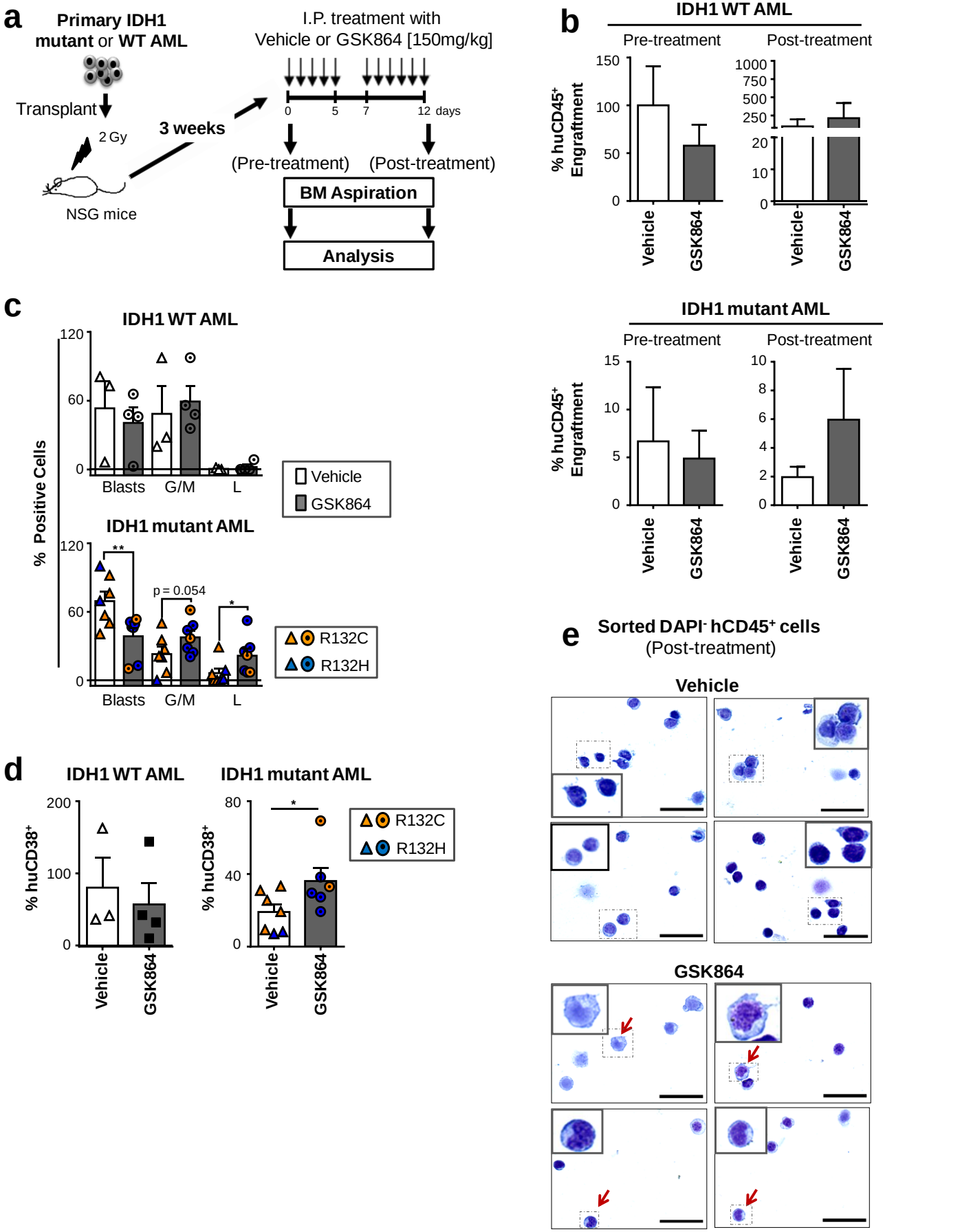


**Supplementary Figure 4**

**Supplementary Figure 4. GSK allosteric IDH1 inhibitor leads to a reduction of primary AML blasts *in vivo*.** (**a**) Schematics of the xenotransplantation of primary wildtype (WT) IDH1, R132C or R132H IDH1-mutant AML cells were transplanted into NSG mice. 3 weeks after transplant (pre-treatment), engrafted cells were assessed by live intrafemoral aspiration and flow cytometric analysis. Engrafted mice are treated with either DMSO vehicle or 150 mg/kg GSK864 over 12 days. Following treatment, bone marrow (BM) aspirates were similarly obtained for flow cytometric analysis. (**b**) Bone marrow AML engraftment levels ($hCD45^{+}$) were determined pre-treatment and post-treatment. Each data point represent individual mouse. Values are represented as mean ± S.E.M. (**c**) Decrease in blasts ($SSC^{low}$ $CD45^{low/+}$), and an increase in cells in the mature G/M (Granulocytic/monocytic) gate upon GSK864 treatment. Analysis was performed after gating on $DAPI^{-}$ $mCD45.1^{-}$ cells. Values are represented as mean ± S.E.M. [Δ vehicle, Θ GSK864, orange - R132C, and blue - R132H] (*p-value < 0.05; **p<0.1). (**d**) Flow cytometric analysis of human CD38 expression on BM cells from mice treated with either vehicle or GSK864. Values are represented as mean ± S.E.M. (**e**) Cell morphological analysis of FACS-sorted viable $DAPI^{-}$ $mCD45.1^{-}$ $huCD45^{+}$ cells. Examples of cells with signs of differentiation are indicated by red arrows. Vehicle control shows majority of cells with typical blast morphology. 50X objective, scale bars 80 μm. Inserts show higher magnification images of the boxed areas. (N = 7 Vehicle treated mice; N = 6 GSK864 treated mice)

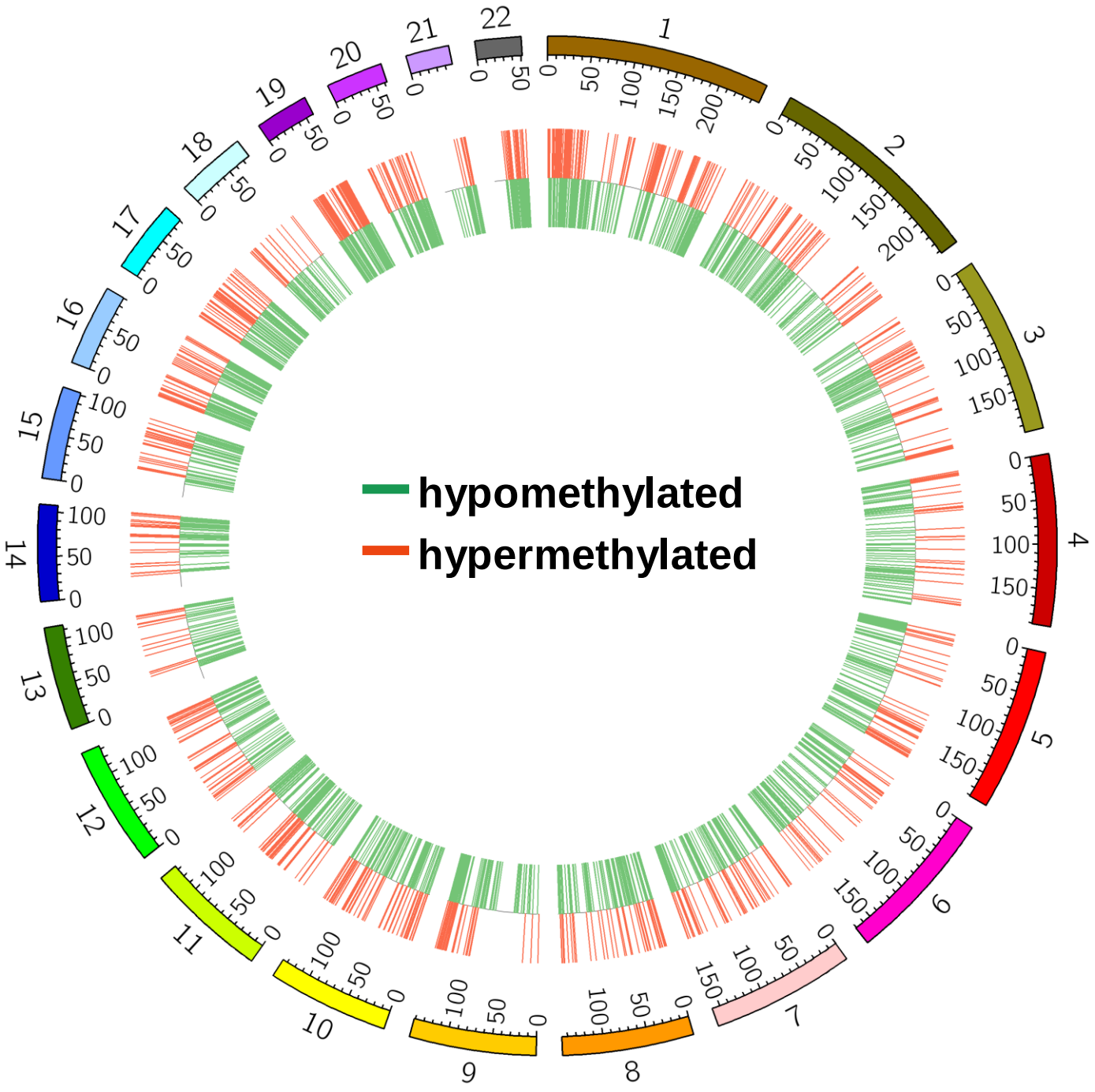


**Supplementary Figure 5**

**Supplementary Figure 5. Genome-wide DNA CpG changes after treatment of IDH1 mutant AML cells with GSK321.** Circos plot depicting hypo- and hypermethylated loci mapped to the different chromosomes. Green bars denote significantly hypomethylated loci; red bars denote significant increase in methylation at the respective loci. Chromosomes are located along the Ideogram.

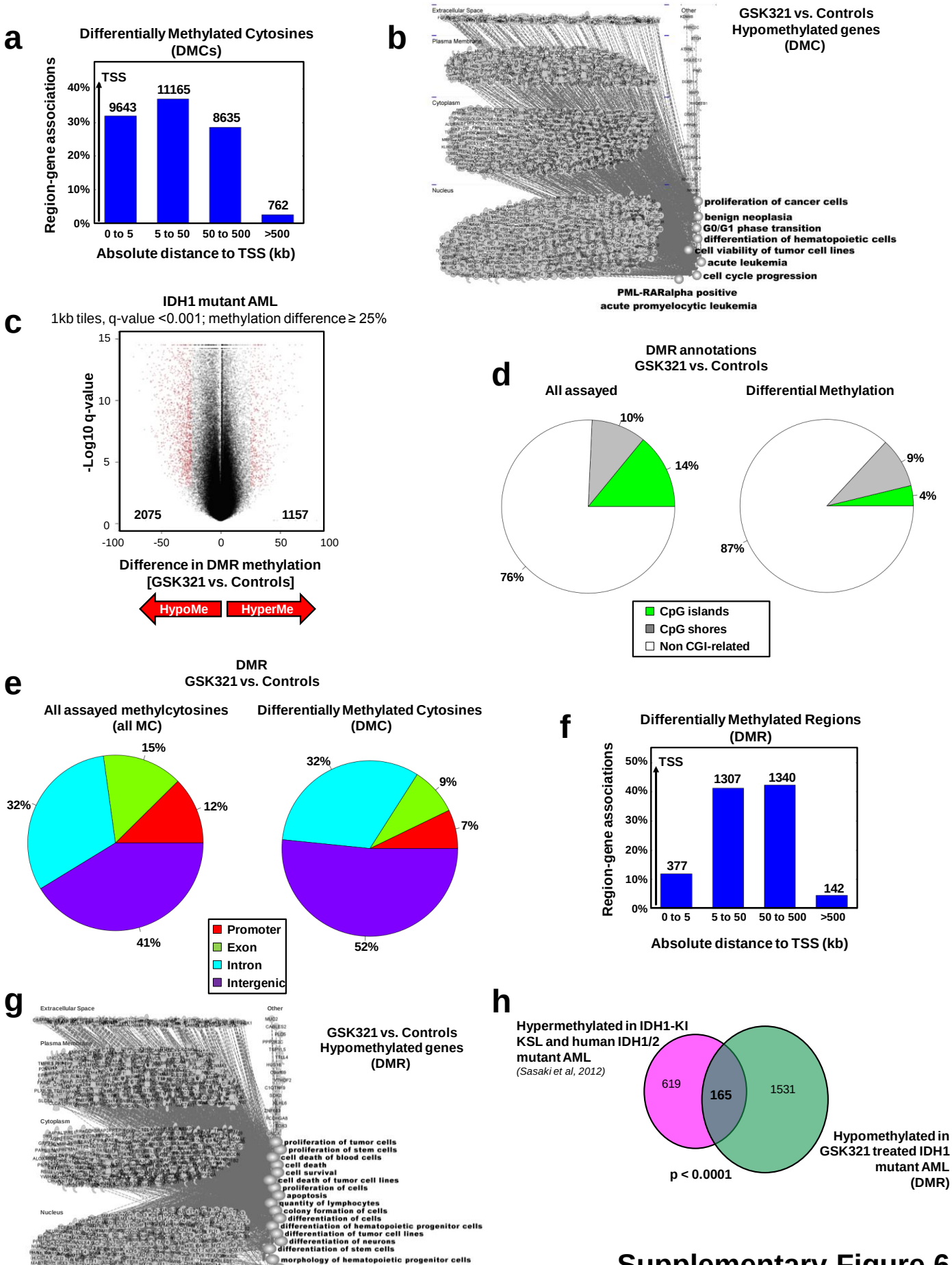


# Supplementary Figure 6

**Supplementary Figure 6. Molecular effects of allosteric mutant IDH1 inhibition.** (**a**) Histogram representing the distance of DMCs to the nearest Transcription Start Site (TSS) following treatment with GSK321 compared to controls. (**b**) Ingenuity pathway analysis of cellular processes encoded by hypomethylated genes (based on DMC) following treatment of IDH1 mutant AML cells with the GSK321 drug. Molecules are organized on the basis of their cellular localization within the extracellular space, plasma membrane, cytoplasm, nucleus or other regions. Hypomethylated genes annotated for q-value < 0.001 and methylation difference ≥ 25% using the Genomic Regions Enrichment of Annotations Tool (GREAT). (**c**) Volcano plot depicting differentially methylated regions (DMRs) (1kb tiles with q-value<0.001 and methylation difference of 25%) [Number of hypomethylated (hypoMe) Loci: 2075; Number of hypermethylated (hyperMe) Loci: 1157]. (**d**) Pie chart illustrating all assayed regions and the proportion of differentially methylated regions (DMRs) annotated to (epi)genomic features upon treatment with GSK321. Green denotes CpG islands, grey denotes CpG shores and white denotes non CGI-related regions. (**e**) Pie chart illustrating all assayed regions and the proportion of differentially methylated regions (DMRs) annotated to promoter regions (red), exons (green), introns (blue) and intergenic regions (purple) throughout the genome. (**f**) Histogram representing the distance of DMRs to the nearest Transcription Start Site (TSS) following treatment with the GSK321 drug compared to controls. (**g**) Ingenuity pathway analysis of cellular processes encoded by hypomethylated DMR genes following treatment of IDH1 mutant AML cells with the GSK321 drug. (**h**) Venn diagram representing the overlap between hypomethylated annotated regions (1696) in GSK321 treated IDH1 mutant AML cells and hypermethylated CpGs (784) in IDH1-knock in (KI) LSK and human IDH1/2 mutant AML. Out of these 784 genes initially hypermethylated in IDH-mutant AML cells, 165 were hypomethylated upon treatment with the active IDH1 inhibitor. p-value < 0.0001.

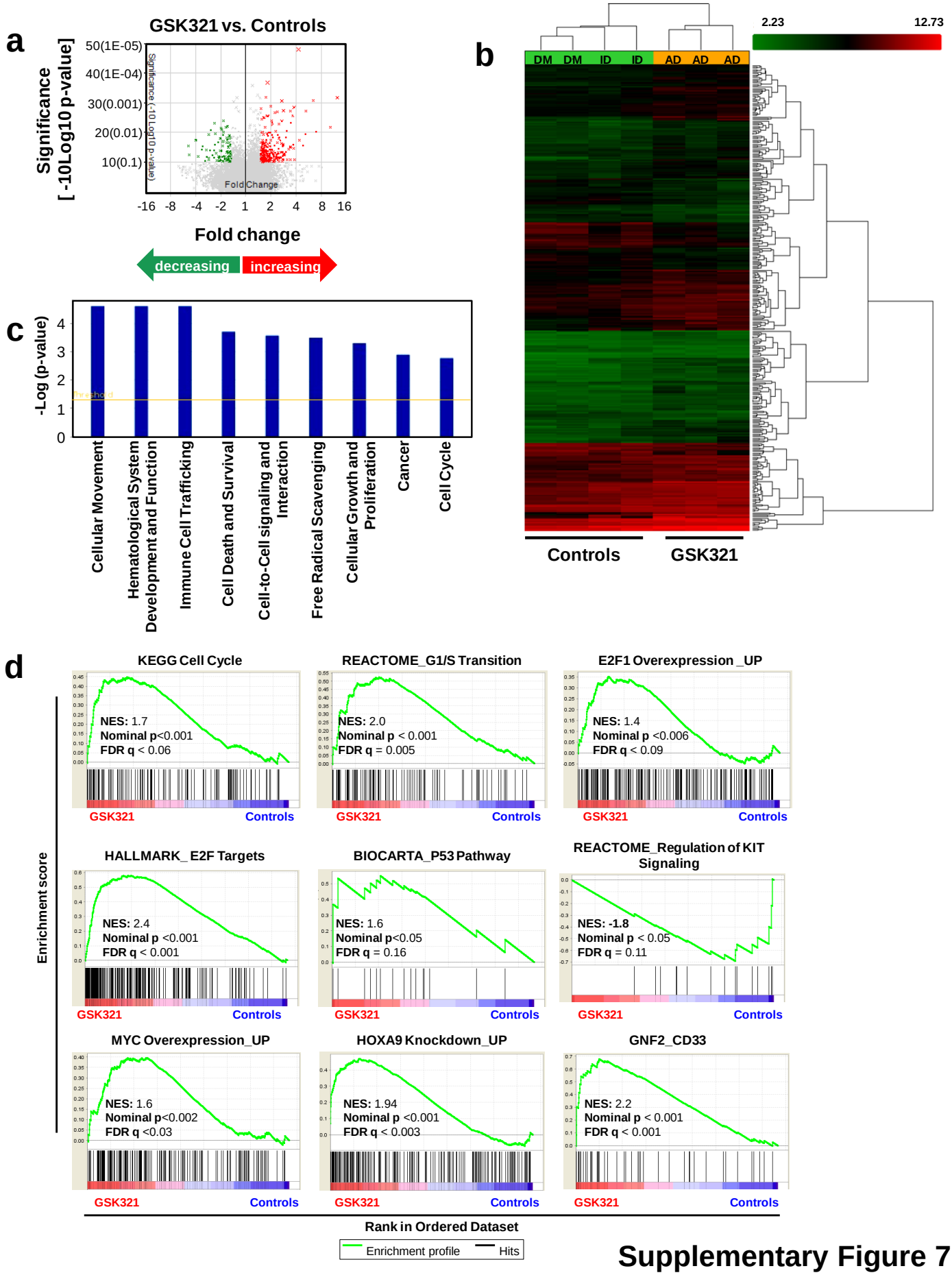


**Supplementary Figure 7**

**Supplementary Figure 7. Transcriptional changes induced by GSK321.** Gene expression microarray analysis was performed on IDH1 mutant AML cells following treatment with either GSK321 (AD - active drug) or DMSO (DM) and GSK990 (ID - inactive drug) controls for 6 days. (N = 3 independent experiments; $p<0.1$, fold change 1.5). (**a**) Volcano plot depicting differentially expressed genes. (**b**) Hierarchical clustering of dysregulated genes. (**c**) IPA gene annotation for the top molecular and cellular functional classes. (**d**) Gene set enrichment analysis (GSEA) was performed and identified transcriptional profiles showing enrichment of genes associated with decreased quiescence, increased cell cycling and proliferation, cell death and cell differentiation.

**Supplementary Information**

# Novel IDH1 Mutant Inhibitors for Treatment of Acute Myeloid Leukemia

Ujunwa C. Okoye-Okafor[1], Boris Bartholdy[1], Jessy Cartier[1], Enoch Gao[2], Beth Pietrak[2], Alan R. Rendina[2], Cynthia Rominger[3], Chad Quinn[2], Angela Smallwood[2], Kenneth J. Wiggall[3], Alexander J. Reif[3], Stanley J. Schmidt[3], Hongwei Qi[2], Huizhen Zhao[2], Gerard Joberty[4], Maria Faelth-Savitski[2], Marcus Bantscheff[4], Gerard Drewes[4], Chaya Duraiswami[2], Pat Brady[2], Arthur Groy[2], Swathi-Rao Narayanagari[1], Ileana Antony-Debre[1], Kelly Mitchell[1], Heng Rui Wang[1], Yun-Ruei Kao[1], Maximilian Christopeit[1], Luis Carvajal[1], Laura Barreyro[1], Elisabeth Paietta[5], Hideki Makishima[6], Britta Will[1], Nestor Concha[2], Nicholas D. Adams[3], Benjamin Schwartz[2], Michael T. McCabe[3], Jaroslav Maciejewski[6], Amit Verma[5,7,8,9], and Ulrich Steidl[1,5,8,9,*]

**Affiliations:**

[1]Department of Cell Biology, Albert Einstein College of Medicine, Bronx, NY, USA

[2]Department of Molecular Discovery Research, GlaxoSmithKline, Collegeville, PA, USA

[3]Cancer Epigenetics Discovery Performance Unit, GlaxoSmithKline, Collegeville, PA, USA

[4]Cellzome, Heidelberg, Germany

[5]Division of Hemato-Oncology, Department of Medicine (Oncology), Albert Einstein College of Medicine / Montefiore Medical Center, Bronx, NY, USA

[6]Taussig Cancer Institute, Cleveland Clinic, Cleveland, OH, United States

[7]Department of Developmental & Molecular Biology, Albert Einstein College of Medicine, Bronx, NY, USA

[8]Albert Einstein Cancer Center, Albert Einstein College of Medicine, Bronx, NY, USA

[9]Gottesman Institute for Stem Cell and Regenerative Medicine Research

*Ulrich Steidl, Albert Einstein College of Medicine, Chanin Bldg. # 601, 1300 Morris Park Avenue, Bronx, NY 10461, ulrich.steidl@einstein.yu.edu.

## Supplementary Results

### Supplementary Tables

**Supplementary Table 1.** Small molecule screening data

| Category | Parameter | Description |
|---|---|---|
| Assay | Type of assay | Biochemical, in vitro assay with a fluorescence intensity readout |
| | Target | Heterodimeric human IDH1 WT/R132H mutant |
| | Primary measurement | Decrease of fluorescence due to inhibition of enzyme activity by test compounds<br><br>The assay measures the oxidative reverse reaction (from 2-hydroxyglutarate (2-HG) to alpha-ketoglutarate(αKG)) catalyzed by the heterodimeric WT/R132H mutant IDH-1 with the concomitant reduction of $NADP^+$ to NADPH. NADPH production is coupled to the diaphorase catalyzed reduction of resazurin to the fluorescent species resorufin.<br><br>Reaction:<br>($NADP^+$) + 2-HG (In presence of IDH-1 WT/R132H) -> αKG+NADPH<br><br>NADPH + resazurin (in presence of diaphorase) -> resorufin |
| | Key reagents | Recombinant human FlagMBP-IDH1 wt/HisMBP-IDH1 R132H heterodimer;<br>2-HG;<br>$NADP^+$;<br>Diaphorase;<br>Resozurin |
| | Assay protocol | 50 nL of test compounds from 1 mM stocks (in 100% DMSO) were pre-stamped into 1536 well black plates. 2 μL of enzyme solution (187 nM R132H/wt IDH1) in base buffer (100 mM Tris, pH=8.0, 10 mM $MgCl_2$, 1 mM |

| | | |
|---|---|---|
| | | CHAPS, 0.1 mg/mL BSA, 0.2 mM DTT) was added to the plate using a Multidrop Combi, excepting control wells in columns 35 and 36 where buffer alone was dispensed. Immediately following, 2 μL of substrate solution (5 mM 2-HG, 7.5 μM $NADP^+$, 25 μM resazurin, 2.5 U/mL diaphorase) in base buffer was added to the entire plate using a second Multidrop Combi. The plates were centrifuged for 1 minute at 500 rpm to ensure mixing and then incubated at room temperature for 2 hours. Reactions were quenched with the addition of 2 μL of stop solution (250 mM EDTA in 100 mM Tris buffer, pH=8.0) added with a third Multidrop Combi, plates were centrifuged a second time as before, and finally read on a Viewlux imager for fluorescence intensity (ex=525nm/em=589nm/561nm dichroic filter). |
| | Additional comments | |
| Library | Library size | 2.14 million compounds |
| | Library composition | 1 mM stock in 100% DMSO; purity >80% (LCMS) |
| | Source | GSK in-house R&D collection and external commercial purchasing |
| | Additional comments | |
| Screen | Format | 1536 well microtiter plate; single dose/singleton compound per well |
| | Concentration(s) tested | 12.5 μM |
| | Plate controls | DMSO (as 0% inhibition); DMSO (and no enzyme) as background control (100% inhibition) |
| | Reagent/ compound dispensing system | Combi Multidrop (Thermo Fisher) with 8 channel dispensing head |
| | Detection instrument and software | Viewlux 1430 imager (PerkinElmer), software version 3.01 SP 2 |
| | Assay validation/QC | Robust Z prime factor >0.6; Signal to background ratio >3.5 |
| | Correction factors | N/A |

| | | |
|---|---|---|
| | Normalization | % inhibition (% reduction of net FLINT signals from test compound comparing to net signals from DMSO controls (with or without enzyme addition) |
| | Additional comments | |
| Post-HTS analysis | Hit criteria | Primary compound responses were corrected via iterative plate pattern detection to reduce systematic plate effects. Compounds with a corrected response exceeding 3 robust SDs above robust mean of test population (22% inhibition, 2.2% hit rate) were marked as primary hits. Property-biased hit marking was also employed to boost identification of ligand efficient hits, yielding a total hit pool of 55k compounds (2.6%). Elimination of weak hits with high MW or cLogP or low efficiency (PEI<1; PEI=10*response/MW) yielded a final list of 26k compounds (1.2%) for confirmation testing. Duplicate confirmation responses and interference testing were utilized to identify 4k compounds for dose response testing. This yielded 1167 compounds with at least on 10uM or better replicate and 96 compounds at 1uM or better. Of eight pyrolopyridines tested in HTS dose response, 6 were 10uM or better and 3 were 1uM or better. |
| | Hit rate | Primary HTS hit rate was 2.2% based upon responses alone, 2.6% including property mined hits, and 1.2% were progressed to confirmation testing. |
| | Additional assay(s) | Confirmation screen of 26k hits from primary screen; primary hits were rescreened under the same assay condition in replicates and single concentration of 12.5 μM.<br><br>XC50 full curve screen for generating full dose-response curves (from 100 μM at top compound dose followed by 11 points 1:2 serial dilution) and pIC50 values. |

| | | |
|---|---|---|
| | | Elimination of compounds which interfere with the coupling system or fluorescence readout. The effects of compounds (single dose or in dose response) on the diaphorase (1 U/mL) coupled conversion of resazurin(10 μM) to resorufin were detected by changes in fluorescence intensity after a 25 minute reaction, using similar detection as the primary IDH1 catalyzed reaction. |
| | Confirmation of hit purity and structure | Confirmed hits after XC50 screen were further purified from solid stocks and re-tested in following assays or analysis:<br>(a) Full dose responses in the same biochemical assay as HTS screen<br>(b) RapidFire-MS based biochemical assay in full dose responses to determine the inhibition of IDH1 mutant enzyme in forward/reductive assay (αKG to 2-HG)<br>(c) Thermal shift assay (Pietrak B. et al, 2011), a biophysical assay to determine the thermal stabilization (Tm shifts) of enzyme resulting from the binding of the compound to the protein<br>(d) Cell based assay to detect the effects (pIC50) of compounds on the 2HG production in HT1080 cell line.<br>(e) Co-crystallization of compound with IDH1 enzyme |
| | Additional comments | |

**Supplementary Table 2.** Biochemical and cellular $IC_{50}$ data for key compounds. Compounds **I-VI** were tested against IDH1 and IDH2 mutant proteins. The chemical structure depicts the backbone of compound. Where R represents modifications to backbone by the addition of the indicated atom or groups.

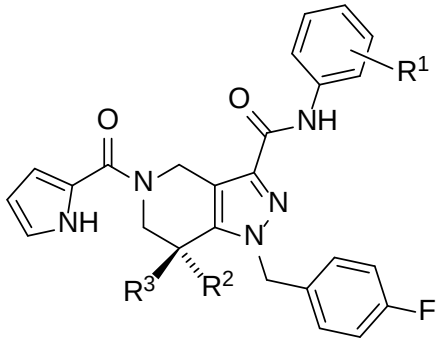


| | Compound | $R^1$ | $R^2$ | $R^3$ | R132H IDH1 $IC_{50}$ (nM) |
|---|---|---|---|---|---|
| | **GSK321** | *(S)*-3-CH(OH)Me | Me | H | 4.6 ± 2.2 |
| | **GSK990** | -- | | | 10915 ± 1761 |
| | **GSK864** | 3,5-di-Me-4-OMe | Me | $C(O)NH_2$ | 15.2 ± 5.1 |
| | **GSK009** | H | H | H | 590 ± 135 |
| | **GSK849** | 3-Me | H | H | 115.1 ± 21.6 |
| | **GSK303** | 3-Me | Me | H | 7.1 ± 2.0 |

**Supplementary Table 3.** Assessment of cell permeability by GSK990, GSK321 and GSK864 as determined by Caco-2 cell permeability assay.

| Caco-2 Permeability | | | | | | | | |
|---|---|---|---|---|---|---|---|---|
| **Test Article** | **Direction** | **Recovery (%)** | **$P_{app}$ ($10^{-6}$ cm/s)** | | | **Efflux Ratio** | **Absorption Potential Classification** | **Significant Efflux** |
| | | | **Rep 1** | **Rep 2** | **Average** | | | |
| GSK990 | A-to-B | 76 | 1.50 | 1.32 | 1.41 | 27 | High | Yes |
| | B-to-A | 71 | 31.0 | 44.0 | 37.5 | | | |
| GSK321 | A-to-B | 51 | 24.0 | 19.9 | 22.0 | 1.4 | High | No |
| | B-to-A | 74 | 26.0 | 33.8 | 29.9 | | | |
| GSK864 | A-to-B | 38 | 27.7 | 29.6 | 28.7 | 1.3 | High | No |
| | B-to-A | 69 | 27.7 | 29.6 | 28.7 | | | |

| | | |
|---|---|---|
| Absorption Potential Classification: | ($P_{app}$ A□B) < 1.0 X $10^{-6}$ cm/s: | **Low** |
| | ($P_{app}$ A□B) ≥ 1.0 X $10^{-6}$ cm/s: | **High** |

| | |
|---|---|
| Significant Efflux: | Efflux Ratio ≥ 2.0 and ($P_{app}$ B□A) ≥ 1.0 X $10^{-6}$ cm/s |

**Supplementary Table 4.** Data collection and refinement statistics of human IDH1 R132H in complex with GSK321

| **Data collection** | |
|---|---|
| **Space group** | P $4_3$ $2_1$ 2 |
| **Molecules in the asymmetric unit** | 2 |
| **Cell dimensions** | |
| ***a*, *b*, *c* (Å)** | 82.7, 82.7, 303.6 |
| **$\alpha$, $\beta$, $\gamma$ (˚)** | 90.0, 90.0, 90.0 |
| **Resolution (Å)** | 30.0 – 2.25 (2.33 – 2.25) |
| **$R_{pim}$ (1)** | 0.026 (0.31) |
| **CC(1/2) (2)** | 0.999 -0.80 |
| ***I*/σ*I*** | 10.1 (3.3) |
| **Completeness (%)** | 99.9 (100.0) |
| **Redundancy** | 8.5 (8.6) |
| | |
| **Refinement** | |
| | |
| **Resolution (Å)** | 2.25 |
| **No. unique reflections** | 51,097 |
| **$R_{work}/R_{free}$** | 0.20/0.25 |
| **No. atoms** | |
| **Protein** | 6235 |
| **$NADP^+$** | 96 |
| **GSK321** | 74 |
| **Water** | 163 |
| **B-factors** | |
| **Protein** | 50.4 |
| **$NADP^+$** | 45.6 |
| **GSK321** | 59.2 |
| **Water** | 48.1 |
| **r.m.s deviations** | |
| **Bond lengths** | 0.004 |
| **Bond angles** | 0.745 |
| **Ramachandran plot (%)** | |
| **Favored** | 97.5 |
| **Allowed** | 2.5 |
| **Disallowed** | 0 |
| | |

Ref 1. M. S. Weiss, Global indicators of x-ray data quality. *J. Appl. Cryst*. **34**, 130-135 (2001)
Ref 2. P. A. Karplus, K. Diedrichs, Linking crystallographic model and data quality. *Science* **336**, 1030-1033 (2012)

**Supplementary Table 5.** Top 5 molecular and cellular functions of hypomethylated annotated genes (Differentially methylated cytosines; q-value <0.001; Methylation difference ≥ 25%)

| Top Molecular and Cellular Functions | p-value | Number of molecules |
|---|---|---|
| **Cellular Growth and Proliferation** | 1.48 E-22 – 4.69E-3 | 1408 |
| **Gene Expression** | 6.65E-16 – 4.86E-3 | 897 |
| **Cellular Movement** | 1.21E-14 – 4.98E-3 | 763 |
| **Cellular Development** | 1.54E-13 – 4.69E-3 | 1060 |
| **Cell Death and Survival** | 2.18E-11 – 5.54E-3 | 1284 |

**Supplementary Table 6.** Enrichment of differentiation and cell fate associated signatures by Gene Ontology (GO) Biological Process analysis of hypomethylated annotated genes using GREAT tool.

| GO Biological Process (hypomethylated genes) | Binomial Bonferroni p-value | Binomial FDR q-value | Hyper FDR q-value |
|---|---|---|---|
| Regulation of monocyte differentiation (GO: 0045655) | 7.79E-5 | 7.18E-4 | 1.21E-1 |
| Positive regulation of hematopoietic progenitor cell differentiation (GO: 1901534) | 7.26E-4 | 5.53E-3 | 9.21E-2 |
| Stem cell fate commitment (GO: 0045880) | 8.95E-3 | 4.77E-2 | 5.12E-2 |
| Ventral spinal cord interneuron fate commitment (GO: 00045880) | 7.70E-12 | 3.30E-10 | 1.32E-2 |
| Regulation of leukocyte degranulation(GO: 0060579) | 4.73E-11 | 1.80E-9 | 1.30E-1 |
| Ventral spinal cord interneuron specification (GO: 0021521) | 7.10E-11 | 2.60E-9 | 2.60E-2 |
| Retinoic acid receptor signaling pathway (GO: 0048384) | 2.55E-6 | 3.68E-5 | 2.24E-2 |
| Positive regulation of smoothened signaling pathway (GO: 0045880) | 1.53E-8 | 3.74E-7 | 8.13E-2 |
| Megakaryocyte differentiation (GO: 0030219) | 5.88E-5 | 6.01E-4 | 6.39E-2 |

**Supplementary Table 7.** Enrichment of differentiation- and cell cycle/cell death- associated signatures as identified by Molecular Signatures Database (MSigDB) perturbation analysis using the GREAT software of all hypomethylated genes. (n.a. not applicable)

| Molecular Signatures Database (MSigDB) Perturbation (hypomethylated genes) | Binomial Bonferroni p-value | Binomial FDR q-value | Hyper FDR q-value |
|---|---|---|---|
| Genes up-regulated from 8-48h during differentiation of 3T3-L1 cells (fibroblasts) into adipocytes | 9.44E-16 | 2.07E-14 | 5.70E-2 |
| Genes up-regulated in NB4 (acute promyelocytic leukemia, APL) in response to tretinoin [PubChem=444795]; based on Chip-seq data | n.a. | n.a. | 7.43E-21 |
| Genes up-regulated by tretinoin (all-trans retinoic acid, ATRA) in U937 cells (acute promyelocytic leukemia, APL) made sensitive to the drug by expression of the PML-RARA fusion | 2.37E-25 | 1.08E-23 | 2.32E-2 |
| Genes with high-CpG density promoters (HCP) bearing the H3K27 tri-methylation (H3K27me3) mark in brain | n.a. | n.a. | 3.53E-44 |
| Cell cycle genes up-regulated in H1299 cells (lung cancer) after overexpression of either P53 or P73 [GeneID=7157;7161] | 1.57E-20 | 4.89E-19 | 9.65E-2 |

**Supplementary Table 8**. Overlapping genes hypomethylated in GSK321 treated IDH1 mutant AML and hypermethylated Lys-M IDH1 mutant Knock-In KSL and human IDH1/2 mutant AML cells. The 784 overlapping hypermethylated genes from *Sasaki et al, Nature 2012* study were compared to the 7339 annotated hypomethylated genes identified after GSK321 treatment of human IDH1 mutant AML cells. A total of 546 genes were identified which were present in both data sets ($p < 0.0001$). All overlapping genes are listed in the table. P-value was determined by Two-tailed Chi-square with Yates' correction.

| | | | | | |
|---|---|---|---|---|---|
| ABAT | COL6A1 | HSPA12A | MYOM2 | RHBDD1 | TOP1 |
| ABCB6 | CRB2 | HSPB1 | MYT1L | RINL | TOR2A |
| ABLIM2 | CRISPLD2 | HTATSF1 | NACC2 | RNF126 | TPO |
| ACOT4 | CTIF | HTR6 | NAT8L | RNF128 | TRIB1 |
| ACTB | CTNND2 | HTR1D | NCOR2 | RNF144A | TRIM2 |
| ACTR3B | CTTN | HTR2C | NCS1 | ROR2 | TRPC4 |
| ACVRL1 | CUX2 | HUNK | NELL1 | RPL38 | TRPM4 |
| ADAD1 | CXCL14 | IER2 | NEUROD2 | RPS6KA4 | TSHZ3 |
| ADAMTS17 | CXCR3 | IGF2BP1 | NEUROG2 | RSPO1 | TSPAN4 |
| ADAMTSL5 | CYP26A1 | IGFBP2 | NFATC2 | RTN1 | TSPAN17 |
| ADCK1 | CYP46A1 | IGSF21 | NFATC4 | RTN4RL1 | UBC |
| ADCY4 | DAGLA | IL16 | NFIC | RUNX3 | UBE2V1 |
| ADCYAP1 | DAP | IL34 | NIPAL4 | RUSC2 | UMODL1 |
| ADORA2A | DAPK2 | IL13RA1 | NKD1 | RXFP3 | UNC13A |
| ADRA2B | DENND3 | IL17D | NKX2-4 | RXRA | UNCX |
| ADRA2C | DHX35 | IQSEC1 | NLGN3 | RYBP | VAMP3 |
| ADRBK1 | DIO2 | IRF8 | NPHP4 | SALL3 | VAX1 |
| AFAP1 | DLGAP4 | IRX1 | NPR1 | SCARB1 | VEGFA |
| AGAP1 | DLL4 | IRX2 | NPVF | SCN1B | VGLL4 |
| AJAP1 | DLX4 | IRX3 | NR2F1 | SDC3 | VPS18 |
| ALX3 | DMRT2 | IRX4 | NR2F2 | SEMA6B | VSTM2L |
| AMN | DMRTB1 | JDP2 | NRK | SEPN1 | WBSCR28 |
| AMPD3 | DNAAF5 | JPH3 | NRP1 | SERPINE1 | WDR34 |
| ANO8 | DNAJB12 | KANK4 | NRP2 | SERTAD2 | WDSUB1 |
| APBB2 | DOCK9 | KCNB1 | NRTN | SEZ6L | WNT3 |
| ARHGAP6 | DPEP1 | KCNC3 | NRXN1 | SHOX2 | WNT5B |
| ARHGAP22 | DPP10 | KCNF1 | NRXN2 | SIGIRR | WNT9B |
| ARHGAP40 | DRD5 | KCNG1 | NTRK2 | SIPA1L2 | WSCD2 |
| ARHGEF3 | DSCAML1 | KCNG4 | NUB1 | SLC15A1 | YKT6 |
| ARHGEF16 | DUSP9 | KCNH2 | NUDT14 | SLC1A3 | ZBP1 |
| ARID1A | EBF2 | KCNJ12 | NUP62CL | SLC1A5 | ZBTB14 |
| ARL10 | EBF3 | KCNK5 | NWD1 | SLC22A3 | ZBTB16 |
| ARX | EEF1A2 | KCNK9 | OBSCN | SLC22A17 | ZBTB7A |
| ASS1 | EFHD2 | KCTD5 | ODC1 | SLC25A47 | ZC3H12A |
| ATAD2B | EFNB1 | KCTD15 | OPCML | SLC28A3 | ZCCHC3 |
| ATP1A3 | EFNB2 | KDM4B | OSBPL10 | SLC30A2 | ZCCHC14 |
| ATP6V0A2 | ELFN2 | KDM6B | OTP | SLC32A1 | ZFAND2A |
| B3GALT4 | EN1 | KIF16B | OTUD5 | SLC35B3 | ZFP64 |
| BAI2 | ENGASE | KIF21A | OTX2 | SLC35D3 | ZFP36L1 |
| BARHL2 | EPAS1 | KIF21B | OXT | SLC6A6 | ZFP36L2 |
| BARX1 | EPHA8 | KIF26A | P2RX2 | SLITRK4 | ZFR2 |

| | | | | | |
|---|---|---|---|---|---|
| BCAR1 | EPS8L2 | KIF26B | PALM3 | SMAD2 | ZIC3 |
| BCL11A | ESM1 | KIRREL2 | PAPOLB | SMAD4 | ZMIZ1 |
| BCL11B | ESR1 | KIRREL | PARVA | SMAD7 | ZMYND8 |
| BCOR | EXOG | KISS1R | PARVG | SMUG1 | ZNRF4 |
| BCORL1 | EYA2 | KLHDC7A | PAX7 | SNAI1 | ZPLD1 |
| BDH1 | F7 | KSR2 | PCDH1 | SNAI2 | |
| BEGAIN | FAM109A | LAPTM4B | PCDH17 | SNX11 | |
| BLK | FAM110A | LARGE | PCDH19 | SNX18 | |
| BMP1 | FAM134B | LBX1 | PCSK9 | SOCS3 | |
| BMP8A | FAM19A5 | LCTL | PDPN | SOX2 | |
| BNC1 | FAT4 | LDLRAP1 | PEBP4 | SOX3 | |
| BOC | FBXO27 | LFNG | PGBD5 | SOX9 | |
| BRF2 | FEZF2 | LHX5 | PGLYRP1 | SOX13 | |
| BRINP1 | FGF6 | LINGO1 | PHF6 | SOX17 | |
| BSX | FGF13 | LMBRD1 | PIK3CD | SPOCK1 | |
| C1QL4 | FIBCD1 | LMO1 | PIM3 | SPON2 | |
| CACNA1B | FLRT2 | LMX1B | PITX1 | SPRED2 | |
| CACNA1G | FMNL1 | LOC102724428/SIK1 | PIWIL1 | SPRY2 | |
| CACNA1I | FOXD1 | LONRF3 | PKN3 | SPSB1 | |
| CACNA2D2 | FOXI2 | LPHN1 | PLXDC1 | SRC | |
| CACNG1 | FOXL1 | LPHN2 | PLXNA4 | SRCIN1 | |
| CACNG8 | FRG1 | LPIN1 | PODXL | SREBF1 | |
| CALN1 | FRMD4A | LRFN2 | POLRMT | SSBP3 | |
| CAMSAP1 | FSCN1 | LRRK1 | POU3F1 | STAB1 | |
| CAMTA1 | FSTL4 | LSR | PRDM12 | STAC2 | |
| CAPG | FXYD4 | LTBP3 | PRDM16 | STOX2 | |
| CAPN13 | FZD2 | LTBP4 | PREX1 | SYT2 | |
| CARTPT | FZD7 | LYNX1 | PRICKLE1 | T | |
| CASZ1 | GABBR2 | MAF | PRICKLE2 | TACC2 | |
| CBLC | GADD45B | MAFA | PRKX | TAF1B | |
| CCDC3 | GALNT6 | MAG | PRMT7 | TBC1D14 | |
| CCNA1 | GAS1 | MAGEE1 | PRPF40B | TBKBP1 | |
| CCNK | GAS7 | MAML3 | PRR5 | TBL1X | |
| CD82 | GATA2 | MAP3K10 | PRRC2B | TBX3 | |
| CD248 | GATA4 | MAST1 | PSAPL1 | TCFL5 | |
| CDC42EP4 | GBX2 | MBNL3 | PTCH1 | TCP11 | |
| CDH4 | GFI1 | MCF2L | PTCHD2 | TEAD1 | |
| CDH5 | GFRA1 | MDGA1 | PTGDR | TEAD4 | |
| CDH20 | GLI2 | MEF2C | PTH1R | TENM4 | |
| CDH22 | GLIS1 | MEGF6 | PTPN18 | TFAP2B | |
| CDKN1C | GLT1D1 | MEN1 | PTPRG | TFAP2C | |
| CELSR1 | GNAS | MEP1B | PTPRM | TGM3 | |
| CERK | GPR84 | MEST | PTPRS | THAP3 | |
| CFD | GPSM1 | MEX3B | PXDN | TIAM1 | |
| CGNL1 | GRIK2 | MFAP2 | PYROXD2 | TMEM53 | |
| CHAD | GRM8 | MGMT | QPRT | TMEM88 | |
| CHD5 | H1F0 | MICAL3 | QRFP | TMEM119 | |
| CHMP4B | H6PD | MID1 | RAB3A | TMEM121 | |

| | | | | | |
|---|---|---|---|---|---|
| CHST1 | HAAO | MKI67 | RAP1GAP | TMEM179 | |
| CHST7 | HABP2 | MMD2 | RARA | TMEM209 | |
| CHST9 | HAND1 | MN1 | RASGEF1C | TMEM106C | |
| CHST11 | HES5 | MORC3 | RBFOX1 | TMEM200B | |
| CILP2 | HIC1 | MPPED1 | RBFOX3 | TNFAIP8 | |
| CKM | HOXA2 | MSI2 | RBM19 | TNFRSF21 | |
| CLDN3 | HOXA5 | MTSS1L | RBMXL2 | TNIK | |
| CLDN14 | HOXD10 | MYCN | RCC2 | TNNI2 | |
| CNKSR2 | HPCA | MYL10 | RCVRN | TNRC18 | |
| CNTN5 | HS3ST2 | MYO16 | RFX4 | TNS3 | |
| COL23A1 | HS6ST1 | MYO7A | RFX8 | TNXB | |

**Supplementary Table 9.** Overlap of hypomethylated and upregulated genes in our study.

| Molecule Name | Entrez Gene ID for Human | Entrez Gene ID for Mouse | Entrez Gene ID for Rat |
|---|---|---|---|
| ACSL1 | 2180 | 14081 | 25288 |
| ADNP2 | 22850 | 240442 | 307236 |
| AFF2 | 2334 | 14266 | 293922 |
| ALDH7A1 | 501 | 110695 | 291450 |
| AZU1 | 566 | | |
| C9orf64 | 84267 | 70153 | 361201 |
| CADM1 | 23705 | 54725 | 363058 |
| CD38 | 952 | 12494 | 25668 |
| CD180 | 4064 | 17079 | 294706 |
| CDC25A | 993 | 12530 | 171102 |
| CKS2 | 1164 | 66197 | 498709 |
| CPD | 1362 | 12874 | 25306 |
| CPM | 1368 | 70574 | 314855 |
| CRYL1 | 51084 | 68631 | 290277 |
| CYBB | 1536 | 13058 | 66021 |
| DDR1 | 780 | 12305 | 25678 |
| DMXL2 | 23312 | 235380 | |
| DZIP1 | 22873 | 66573 | 364475 |
| EDA2R | 60401 | 245527 | 296872 |
| ELANE | 1991 | 50701 | 299606 |
| F3 | 2152 | 14066 | 25584 |
| FAM174A | 345757 | 67698 | 301634 |
| FAM198B | 51313 | 68659 | 310540 |
| FBN2 | 2201 | 14119 | 689008 |
| FCGR1B | 2210 | | |
| FNDC3B | 64778 | 72007 | 294925 |
| FOSL2 | 2355 | 14284 | |
| FOXC1 | 2296 | 17300 | 364706 |
| GPNMB | 10457 | 93695 | 113955 |
| GPR64 | 10149 | 237175 | 266735 |
| HAL | 3034 | 15109 | 29301 |
| IFI30 | 10437 | 65972 | 290644 |
| LONRF3 | 79836 | 74365 | 298322 |
| LY86 | 9450 | 17084 | 291359 |
| LYST | 1130 | 17101 | 85419 |
| MPO | 4353 | 17523 | |
| MS4A6A | 64231 | 68774 | 361735 |
| MYC | 4609 | 17869 | 24577 |
| NEIL3 | 55247 | 234258 | 290729 |
| P2RY2 | 5029 | 18442 | 29597 |
| PM20D2 | 135293 | 242377 | 313130 |
| S100B | 6285 | 20203 | 25742 |
| SELRC1 | 65260 | 69893 | 298377 |
| SERPINB2 | 5055 | 18788 | 60325 |
| SLC25A37 | 51312 | 67712 | 306000 |

| | | | |
|---|---|---|---|
| SLC46A3 | 283537 | 71706 | 288454 |
| SLCO4C1 | 353189 | 227394 | 432363 |
| SLMO1 | 10650 | 225655 | 690253 |
| SNX18 | 112574 | 170625 | 310097 |
| SPATA9 | 83890 | 75571 | 294594 |
| SRGN | 5552 | 19073 | 56782 |
| STEAP4 | 79689 | 117167 | 499991 |
| STOX2 | 56977 | 71069 | 306459 |
| TAGAP | 117289 | 72536 | 308097 |
| TEX35 | 84066 | 73435 | 680164 |
| TLDC1 | 57707 | 74347 | 307901 |
| TLR4 | 7099 | 21898 | 29260 |
| TMEM168 | 64418 | 101118 | 312135 |
| TMEM170B | 100113407 | 621976 | 361230 |
| TRERF1 | 55809 | 224829 | |
| TUBB6 | 84617 | 67951 | 307351 |
| UACA | 55075 | 72565 | |
| WDFY1 | 57590 | 69368 | |
| ZNF711 | 7552 | 245595 | 302327 |
| ZNF804A | 91752 | 241514 | 295695 |

**Supplementary Table 10.** Primer sequences

| Identifier | Sequence (5'→3') | Annealing Temperature | Use | Reference |
|---|---|---|---|---|
| **IDH1 FW1** | TGCCACCAACGACCAAGTCA | 59.5°C | For PCR amplification of IDH1 Exon 4 | Wagner et al, 2010 |
| **IDH1 RV1** | TGTGTTGAGATGGACGCCTATTTG | | | |
| **IDH1 FW2** | ACCAAATGGCACCATACGA | 54.4°C | For nested PCR amplification of IDH1 Exon 4 | Lu et al, 2012 |
| **IDH1 RV2** | TTCATACCTTGCTTAATGGGTGT | | | |
| **IDH2 FW1** | GGGGTTCAAATTCTGGTTGA | 53°C | For PCR amplification of IDH2 Exon 4 | Liang DC et al, 2013 |
| **IDH2 RV1** | TGTGGCCTTGTACTGCAGAG | | | |
| **IDH2 FW2** | AAGATGGCGGCTGCAGTGGG | 63.2°C | For nested PCR | ---- |

| | | | | |
|---|---|---|---|---|
| **IDH2 RV2** | AGGCGAGGAGCTCCAGTCGG | | amplification of IDH2 Exon 4 | |

**Supplementary Table 11.** Somatic events in the IDH1 mutant samples utilized in the study.

| | Sample | Co-mutations |
|---|---|---|
| **1.** | R132C | IDH1; DNMT3A; NPM1 |
| **2.** | R132G | IDH1; NPM1 (FS); WT (G60R) |
| **3.** | R132G | IDH1 |
| **4.** | R132H | IDH1; DNMT3A; FLT3; PTPPN11; |
| **5.** | R132G | IDH1; DNMT3A (L647P; R771X) |
| **6.** | R132C | IDH1 |
| **7.** | R132H | IDH1; DNMT3A (Q816X); FLT3-ITD; NPM1 (FS); NRAS (G13D) |
| **8.** | R132H | IDH1; NPM1; PHF6; NF1; U2AF1 |
| **9.** | R132H | IDH1; DHX29; JAK2; |
| **10.** | R132C | IDH1 |
| **11.** | R132C | IDH1; DNMT3A (R882H) |
| **12.** | R132H | IDH1 |
| **13.** | R132C | IDH1; PTEN (R142W); NPM1 (FS) |
| **14.** | R132H | IDH1; DNMT3A (R882H); NPM1 (FS); KRAS (G13D); RUNX1 (FS135) |

**Supplementary Data Set 1 –** Chemoproteomic approach showing selectivity of GSK321 for IDH1 [QUP, quantified unique peptides]

**Supplementary Data Set 2 –** Differentially expressed genes by microarray analysis

**Supplementary Notes** – Compound Synthesis

**Supplementary Notes:**

## Compound synthesis

### Synthesis of GSK009 (5) and GSK849 (3) [a]

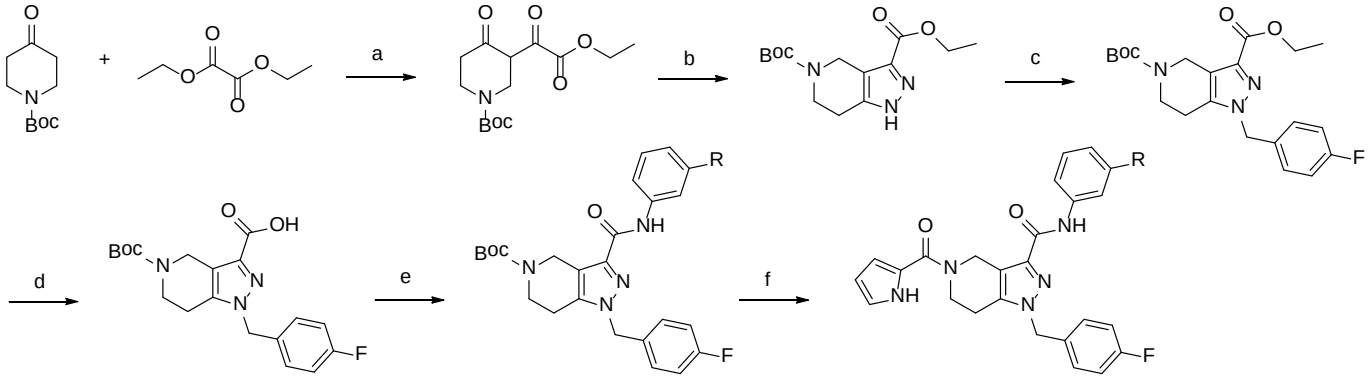

[a]Reagents and Conditions: (a) LDA, THF, -78 °C; (b) hydrazine hydrate, AcOH; (c) NaH, 1-(bromomethyl)-4-fluorobenzene, THF; (d) NaOH, EtOH, water; (e) aniline for **GSK009** or m-toluidine for **GSK849**, HATU, i-$Pr_2$NEt, DCM; (f) 4N HCl in dioxane, DCM; then 1*H*-pyrrole-2-carboxylic acid, HATU, i-$Pr_2$NEt, DCM.

### 1-[(4-fluorophenyl)methyl]-*N*-phenyl-5-(1*H*-pyrrol-2-ylcarbonyl)-4,5,6,7-tetrahydro-1*H*-pyrazolo[4,3-*c*]pyridine-3-carboxamide (GSK009)

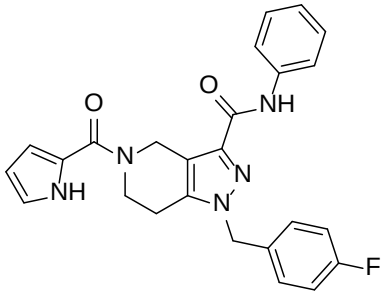

### Step a) *tert*-butyl 3-(2-ethoxy-2-oxoacetyl)-4-oxopiperidine-1-carboxylate (7)

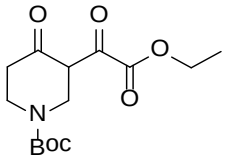

To a solution of *tert*-butyl 4-oxopiperidine-1-carboxylate (20 g, 100 mmol) in THF (250 mL) was added a solution of 2M LDA in THF (57.5 mL, 115 mmol) at -78 °C, the

mixture was stirred at -78 °C for one hour and a solution of diethyl oxalate (17.7 g, 121 mmol) in THF (50 mL) was added. The resulting mixture was allowed to warm to room temperature, stirred overnight and water (500 mL) was added. The aqueous phase was neutralized with 1 N HCl and extracted with EtOAc (500 mL). The organic layer was washed with brine (500 mL), dried over $Na_2SO_4$, concentrated under reduced pressure and the residue was purified by silica gel chromatography (PE : EtOAc = 3 : 1) to give *tert*-butyl 3-(2-ethoxy-2-oxoacetyl)-4-oxopiperidine-1-carboxylate (15.5 g, 51.9 mmol, 51.8 % yield) as a yellow oil. NMR analysis shows ~0.34 equivalents of EtOAc that could not be removed. $MS(ES)^+$ m/e 244.1 $[MH-55]^+$. $^1H$ NMR (300 MHz, $CDCl_3$) $\delta$ 15.35 (br. s., 1H), 4.45 (s, 2H), 4.35 (q, *J* = 7.2 Hz, 2H), 3.65 (t, *J* = 6.0 Hz, 2H), 2.58 (t, *J* = 6.0 Hz, 2H), 1.47 (s, 9H), 1.39 (t, *J* = 7.2 Hz, 3H).

**Step b) 5-*tert*-butyl 3-ethyl 6,7-dihydro-1*H*-pyrazolo[4,3-*c*]pyridine-3,5(4*H*)-dicarboxylate (8)**

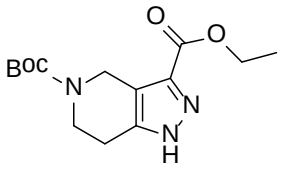


To a solution of *tert*-butyl 3-(2-ethoxy-2-oxoacetyl)-4-oxopiperidine-1-carboxylate (15.5 g, 51.9 mmol) in $CH_3COOH$ (40 mL) was added hydrazine hydrate (4 mL, 124 mmol) portionwise. The mixture was stirred at room temperature overnight then poured into ice cold saturated aqueous sodium bicarbonate and extracted with EtOAc (800 mL). The organic extract was washed with brine (800 mL), dried over $Na_2SO_4$, filtered, concentrated under reduced pressure and the residue was purified by silica gel chromatography (PE : EtOAc = 3 : 1) to give 5-*tert*-butyl 3-ethyl 6,7-dihydro-1*H*-pyrazolo[4,3-*c*]pyridine-3,5(4*H*)-dicarboxylate (13.7 g, 46.4 mmol, 89.5% yield) as a white solid. $MS(ES)^+$ m/e 296.1 $[M+H]^+$. $^1H$ NMR (300 MHz, $CDCl_3$) $\delta$ ppm 4.64 (s, 2H), 4.37 (q, *J* = 6.9 Hz, 2H), 3.71 (s, 2H), 2.82 (t, *J* = 5.4 Hz, 2H), 1.49 (s, 9H), 1.38 (t, *J* = 6.9 Hz, 3H).

**Step c) 5-*tert*-butyl 3-ethyl 1-(4-fluorobenzyl)-6,7-dihydro-1*H*-pyrazolo[4,3-*c*]pyridine-3,5(4*H*)-dicarboxylate (9)**

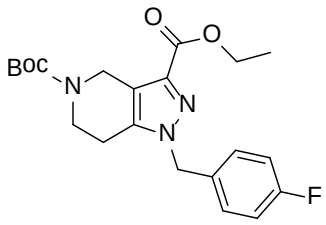


To a solution of 5-*tert*-butyl 3-ethyl 6,7-dihydro-1*H*-pyrazolo[4,3-*c*]pyridine-3,5(4*H*)-dicarboxylate (10 g, 33.9 mmol) in THF (150 mL) was slowly added NaH (1.63

g, 40.6 mmol) at room temperature. After 1 hour, a solution of 1-(bromomethyl)-4-fluorobenzene (6.72 g, 35.6 mmol) in THF (5 mL) was added and the mixture was stirred at room temperature overnight. The reaction mixture was quenched with water (100 mL) and the aqueous layer was extracted with EtOAc (300 mL). The organic layer was washed with brine (200 mL), dried over $Na_2SO_4$, filtered and concentrated under reduced pressure. The residue was purified by silica gel chromatography (PE : EtOAc = 2 : 1) to provide 5-*tert*-butyl 3-ethyl 1-(4-fluorobenzyl)-6,7-dihydro-1*H*-pyrazolo[4,3-*c*]pyridine-3,5(4*H*)-dicarboxylate compound (6.8 g, 16.8 mmol, 50 % yield) as a yellow oil. MS(ES)$^+$ m/e 404.1 $[M+H]^+$. $^1$H NMR (300 MHz, $CDCl_3$) $\delta$ ppm 7.12 - 7.17 (m, 2H), 6.98 - 7.04 (m, 2H), 5.30 (s, 2H), 4.61 (s, 2H), 4.41 (q, *J* = 7.2 Hz, 2H), 3.65 (d, *J* = 4.8 Hz, 2H), 2.52 (s, 2H), 1.47 (s, 9H), 1.40 (t, *J* = 7.2 Hz, 3H).

**Step d) 5-(*tert*-butoxycarbonyl)-1-(4-fluorobenzyl)-4,5,6,7-tetrahydro-1*H*-pyrazolo[4,3-*c*]pyridine-3-carboxylic acid (10)**

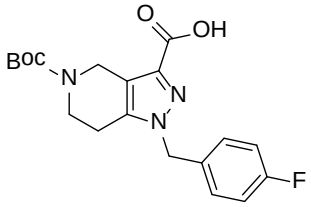


To a solution of 5-*tert*-butyl 3-ethyl 1-(4-fluorobenzyl)-6,7-dihydro-1*H*-pyrazolo[4,3-*c*]pyridine-3,5(4*H*)-dicarboxylate (4.03 g, 10 mmol) in EtOH (40 mL) was added NaOH (0.8 g, 20 mmol) in water (20 mL). The resulting mixture was stirred at room temperature for 4 hours, concentrated under reduced pressure, diluted with water (40 mL) and washed with EtOAc (100 mL). The pH of the aqueous layer was adjusted to 6 with 1 N HCl and the resulting precipitate was collected by filtration and dried to give 5-(*tert*-butoxycarbonyl)-1-(4-fluorobenzyl)-4,5,6,7-tetrahydro-1*H*-pyrazolo[4,3-*c*]pyridine-3-carboxylic acid (2.82 g, 7.52 mmol, 75 % yield) as a white soild. MS(ES)$^+$ m/e 376.1 $[M+H]^+$. $^1$H NMR (400 MHz, DMSO-$d_6$) $\delta$ ppm 12.75 (bs, 1 H), 7.22 - 7.34 (m, 2 H), 7.12 - 7.22 (m, 2 H), 5.31 (s, 2 H), 4.46 (s, 2 H), 3.58 (t, *J* = 5.68 Hz, 2 H), 2.63 (t, *J* = 5.56 Hz, 2 H), 1.40 (s, 9 H).

**Steps e & f) 1-[(4-fluorophenyl)methyl]-*N*-phenyl-5-(1*H*-pyrrol-2-ylcarbonyl)-4,5,6,7-tetrahydro-1*H*-pyrazolo[4,3-*c*]pyridine-3-carboxamide (GSK009)**

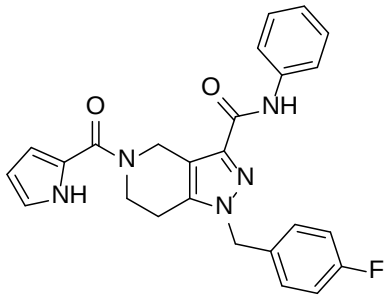


To a vial, 5-(*tert*-butoxycarbonyl)-1-(4-fluorobenzyl)-4,5,6,7-tetrahydro-1*H*-pyrazolo[4,3-*c*]pyridine-3-carboxylic acid (222 mg, 0.591 mmol) and 2-(3*H*-[1,2,3]triazolo[4,5-b]pyridin-3-yl)-1,1,3,3-tetramethylisouronium hexafluorophosphate(V) (281 mg, 0.739 mmol) were combined and suspended in DCM (9 mL). Aniline (68.8 mg, 0.739 mmol) and i-$Pr_2$NEt (191 mg, 1.478 mmol) were added to the mixture. The solution was stirred at room temperature for 2 hours and LCMS analysis indicated desired amide formation. The mixture was added to a separatory funnel containing water and was extracted with DCM (3x). The combined organics were dried over sodium sulfate, filtered, and concentrated to an oil that was carried forward without purification.

To a vial, crude tert-butyl 1-(4-fluorobenzyl)-3-(phenylcarbamoyl)-6,7-dihydro-1*H*-pyrazolo[4,3-*c*]pyridine-5(4*H*)-carboxylate (265 mg, 0.588 mmol) was dissolved in DCM (9 mL) and HCl (2 mL, 8.0 mmol; 4N HCl in 1,4-dioxane) was added. The mixture was stirred at room temperature for 30 minutes and LCMS analysis indicated protecting group cleavage. The solution was concentrated *in vacuo* and the residue was redissolved in DCM (10 mL). DIPEA (76 mg, 0.587 mmol), HATU (223 mg, 0.587 mmol), and 1*H*-pyrrole-2-carboxylic acid (65.2 mg, 0.587 mmol were added and the mixture was stirred at room temperature for 2 hours. LCMS analysis indicated desired product and the mixture was concentrated. This material was purified on silica gel (24g column, 25-50-100 % EtOAc/Hexanes). The desired fractions were concentrated to yield a tan solid that was re-purified on reverse phase HPLC (15-80 % acetonitrile/water with 0.1 % $NH_4OH$). The desired fractions were concentrated to afford the desired product as a white solid, 1-(4-fluorobenzyl)-*N*-phenyl-5-(1*H*-pyrrole-2-carbonyl)-4,5,6,7-tetrahydro-1*H*-pyrazolo[4,3-*c*]pyridine-3-carboxamide (200 mg, 77 %). MS(ES)$^+$ m/e 444.3 $[M+H]^+$. $^1$H NMR (400 MHz, DMSO-$d_6$) $\delta$ ppm 11.54 (br. s., 1 H), 10.05 (s, 1 H), 7.82 (d, *J* = 7.83 Hz, 2 H), 7.25 - 7.38 (m, 4 H), 7.14 - 7.25 (m, 2 H), 7.02 - 7.13 (m, 1 H), 6.91 (d, *J* = 1.01 Hz, 1 H), 6.57 (br. s., 1 H), 6.13 - 6.21 (m, 1 H), 5.42 (s, 2 H), 4.94 (br. s., 2 H), 3.92 (br. s., 2 H), 2.79 (br. s., 2 H). $^{13}$C NMR spectra generally complex for this series due to presence of rotamers and $^{19}$F splitting. $^{13}$C NMR (100.61 MHz, $CDCl_3$) 164.61, 163.76, 161.30, 160.18, 140.83, 139.20, 137.70, 131.28, 129.12, 128.99, 128.94, 128.79, 128.71, 124.44, 124.28, 124.03, 121.84, 121.20, 119.85, 116.73, 116.25, 116.03, 109.99, 52.90, 44.21, 40.29, 22.04.

**1-[(4-fluorophenyl)methyl]-*N*-(3-methylphenyl)-5-(1*H*-pyrrol-2-ylcarbonyl)-4,5,6,7-tetrahydro-1*H*-pyrazolo[4,3-*c*]pyridine-3-carboxamide (GSK849)**

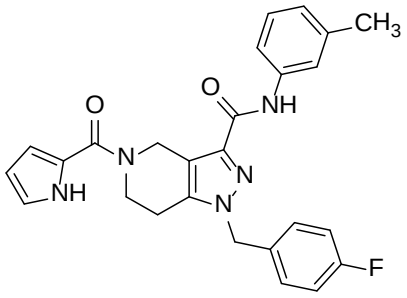

The procedure described for the preparation of **GSK009** was followed replacing aniline with *m*-toluidine which provided the title compound **GSK849** as a white solid (40 mg, 15 %). MS(ES)$^+$ m/e 458.3 $[M+H]^+$. $^1$H NMR (400 MHz, DMSO-$d_6$) $\delta$ ppm 11.53 (br. s., 1 H), 9.91 (s, 1 H), 7.70 (s, 1 H), 7.57 (d, $J$ = 8.08 Hz, 1 H), 7.26 - 7.41 (m, 2 H), 7.12 - 7.26 (m, 3 H), 6.84 - 6.96 (m, 2 H), 6.57 (br. s., 1 H), 6.11 - 6.24 (m, 1 H), 5.41 (s, 2 H), 4.93 (br. s., 2 H), 3.91 (br. s., 2 H), 2.79 (br. s., 2 H), 2.30 (s, 3 H). $^{13}$C NMR spectra generally complex for this series due to presence of rotamers and $^{19}$F splitting. $^{13}$C NMR (100.61 MHz, $CDCl_3$) 163.77, 162.57, 161.31, 160.13, 140.90, 139.19, 138.99, 137.63, 131.29, 129.37, 129.00, 128.80, 128.74, 125.03, 124.52, 121.67, 121.03, 120.41, 120.23, 116.92, 116.71, 116.26, 116.03, 110.03, 52.91, 44.21, 22.03, 21.56, 21.52.

**Synthesis of compounds GSK303 (6) and GSK321 (1)** [a]

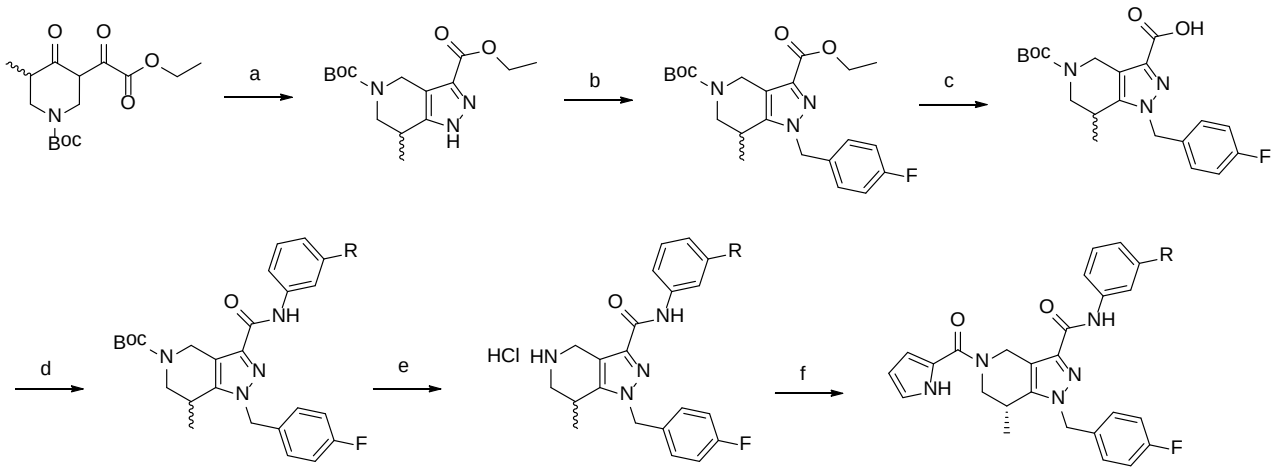

[a]Reagents and Conditions: (a) hydrazine hydrate, AcOH; (b) NaH, 1-(bromomethyl)-4-fluorobenzene, THF; (c) NaOH, EtOH, water; (d) *m*-toluidine, HATU, i-$Pr_2$NEt, DCM for **GSK303**; or 1-(3-aminophenyl)ethanol, HOBt, EDC, i-$Pr_2$Net, THF for **GSK321**; (e) 4N HCl in dioxane, DCM; f) 1*H*-pyrrole-2-carboxylic acid, HATU, i-$Pr_2$NEt, DCM for **GSK303**; or 1*H*-pyrrole-2-carboxylic acid, HOBt, EDC, i-$Pr_2$NEt, THF for **GSK321**; then chiral prep HPLC.

**(7*R*)-1-[(4-fluorophenyl)methyl]-7-methyl-*N*-(3-methylphenyl)-5-(1*H*-pyrrol-2-ylcarbonyl)-4,5,6,7-tetrahydro-1*H*-pyrazolo[4,3-*c*]pyridine-3-carboxamide (GSK303)**

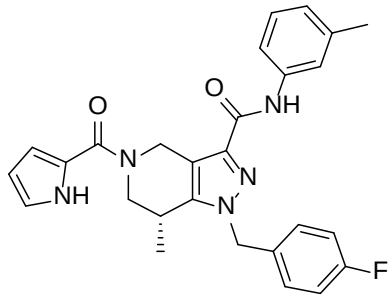

**Step a) 5-*tert*-butyl 3-ethyl 7-methyl-6,7-dihydro-1*H*-pyrazolo[4,3-*c*]pyridine-3,5(4*H*)-dicarboxylate (11)**

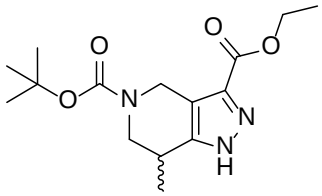

To a solution of *tert*-butyl 3-(2-ethoxy-2-oxoacetyl)-5-methyl-4-oxopiperidine-1-carboxylate (1.25 g, 3.99 mmol) in acetic acid (5 mL) was added hydrazine hydrate (0.469 mL, 9.57 mmol). After 1 hour, the reaction mixture was concentrated under reduced pressure and the residue was diluted with water and saturated aqueous $NaHCO_3$ and extracted with two portions of EtOAc. The combined extracts were dried over $Na_2SO_4$, filtered, concentrated under reduced pressure and dried to constant weight to provide 5-*tert*-butyl 3-ethyl 7-methyl-6,7-dihydro-1*H*-pyrazolo[4,3-*c*]pyridine-3,5(4*H*)-dicarboxylate (1.14 g, 3.69 mmol, 92 % yield) as a pale yellow solid. $MS(ES)^+$ m/e 310.2 $[M+H]^+$. $^1H$ NMR (400 MHz, DMSO-$d_6$) $\delta$ ppm 13.18-13.90 (m, 1H), 4.35 - 4.74 (m, 2H), 4.27 (d, *J* = 5.56 Hz, 2H), 3.60-3.91 (m, 1H), 3.00 - 3.28 (m, 1H), 2.93 (br. s., 1H), 1.42 (s, 9H), 1.25 - 1.33 (m, 3H), 1.11 - 1.21 (m, 3H).

**Step b) 5-*tert*-butyl 3-ethyl 1-(4-fluorobenzyl)-7-methyl-6,7-dihydro-1*H*-pyrazolo[4,3-*c*]pyridine-3,5(4*H*)-dicarboxylate (12)**

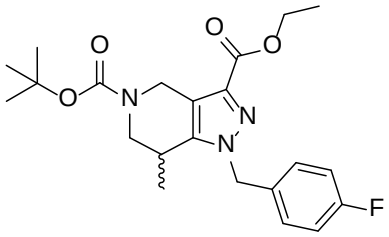

To a solution of 5-*tert*-butyl 3-ethyl 7-methyl-6,7-dihydro-1*H*-pyrazolo[4,3-*c*]pyridine-3,5(4*H*)-dicarboxylate (1.13 g, 3.65 mmol) in dry THF (17 mL) was added NaH (60 % wt dispersion in mineral oil, 0.175 g, 4.38 mmol) with stirring under nitrogen. After 1 hour, 1-(bromomethyl)-4-fluorobenzene (0.690 g, 3.65 mmol) was added and the reaction mixture was stirred overnight (15 h) under nitrogen. The reaction mixture was quenched with water and the pH adjusted to ~6 with 1N HCl. The mixture was diluted with brine and extracted with two portions of EtOAc. The combined extracts were dried over $Na_2SO_4$, filtered and concentrated under reduced pressure. The residue was purified by silica gel chromatography (Analogix, SF25-40 g column, 30-40 % EtOAc in hexanes). The appropriate fractions were combined, concentrated under reduced pressure and the residue was dried to constant weight under high vacuum to provide 5-*tert*-butyl 3-ethyl 1-(4-fluorobenzyl)-7-methyl-6,7-dihydro-1*H*-pyrazolo[4,3-*c*]pyridine-3,5(4*H*)-dicarboxylate (1.14 g, 2.73 mmol, 74 % yield) as a white solid. MS(ES)$^+$ m/e 418.5 $[M+H]^+$. $^1$H NMR (400 MHz, DMSO-$d_6$) $\delta$ ppm 7.11 - 7.25 (m, 4H), 5.27 - 5.52 (m, 2H), 4.73 - 5.07 (m, 1H), 3.80 - 4.35 (m, 4H), 2.98 - 3.25 (m, 2H), 1.42 (s, 9H), 1.29 (t, *J* = 7.07 Hz, 3H), 1.01 (br. s., 3H).

**Step c) 5-(*tert*-butoxycarbonyl)-1-(4-fluorobenzyl)-7-methyl-4,5,6,7-tetrahydro-1*H*-pyrazolo[4,3-*c*]pyridine-3-carboxylic acid (13)**

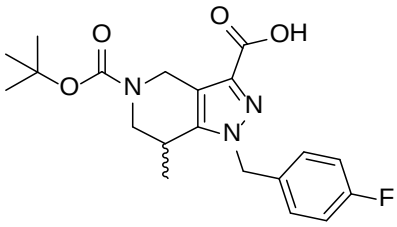

To a solution of 5-*tert*-butyl 3-ethyl 1-(4-fluorobenzyl)-7-methyl-6,7-dihydro-1*H*-pyrazolo[4,3-*c*]pyridine-3,5(4*H*)-dicarboxylate (1.13 g, 2.71 mmol) in ethanol (15 mL) was added 1N NaOH (5.4 mL, 5.4 mmol). The clear solution was stirred at room temperature. After 2 hours the reaction was judged complete by LCMS. The EtOH was removed under reduced pressure and the residue was diluted with water and pH adjusted to ~6 with 1N HCl. The resulting precipitate was collected by filtration and dried on a lyophilizer overnight to provide 5-(*tert*-butoxycarbonyl)-1-(4-fluorobenzyl)-7-methyl-4,5,6,7-tetrahydro-1*H*-pyrazolo[4,3-*c*]pyridine-3-carboxylic acid (485 mg, 1.245 mmol) as a white solid. MS(ES)$^+$ m/e 390.2 $[M+H]^+$. The filtrate left from the filtration was extracted with four portions of EtOAc and the combined extracts were dried over $Na_2SO_4$, filtered and concentrated under reduced pressure. The residue was dried to

constant weight under high vacuum to provide a second portion of 5-(*tert*-butoxycarbonyl)-1-(4-fluorobenzyl)-7-methyl-4,5,6,7-tetrahydro-1*H*-pyrazolo[4,3-*c*]pyridine-3-carboxylic acid (480 mg, 1.233 mmol) as a white solid. $MS(ES)^+$ m/e 390.2 $[M+H]^+$. $^1H$ NMR (400 MHz, DMSO-$d_6$) $\delta$ ppm 7.01 - 7.31 (m, 4H), 5.21 - 5.44 (m, 2H), 4.74 - 5.04 (m, 1H), 3.74 - 4.22 (m, 2H), 2.89 - 3.19 (m, 2H), 1.41 (s, 9H), 1.00 (br. s., 3H).

**Step d) *tert*-butyl 1-(4-fluorobenzyl)-7-methyl-3-(*m*-tolylcarbamoyl)-6,7-dihydro-1*H*-pyrazolo[4,3-c]pyridine-5(4*H*)-carboxylate (14)**

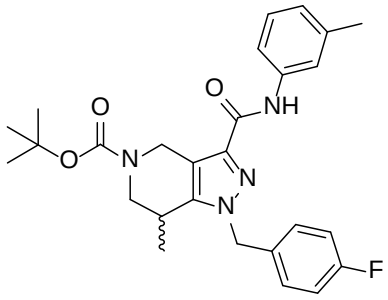


To a solution of 5-(*tert*-butoxycarbonyl)-1-(4-fluorobenzyl)-7-methyl-4,5,6,7-tetrahydro-1*H*-pyrazolo[4,3-*c*]pyridine-3-carboxylic acid (0.48 g, 1.23 mmol) in DCM (12 mL) were added *m*-toluidine (0.147 mL, 1.35 mmol), HATU (0.703 g, 1.85 mmol) and i-$Pr_2NEt$ (0.431 mL, 2.47 mmol). The mixture was stirred at room temperature under nitrogen. After 3 hours, the reaction mixture was quenched with water and the aqueous layer was extracted with two portions of DCM. The combined DCM extracts were dried over $Na_2SO_4$, filtered and concentrated under reduced pressure. The residue was purified by silica gel chromatography (Analogix, SF25-40 g column, 35 % EtOAc in hexanes). The appropriate fractions were combined, concentrated under reduced pressure and the residue was dried to constant weight under high vacuum to provide *tert*-butyl 1-(4-fluorobenzyl)-7-methyl-3-(*m*-tolylcarbamoyl)-6,7-dihydro-1*H*-pyrazolo[4,3-c]pyridine-5(4*H*)-carboxylate (0.563 g, 1.176 mmol, 95 % yield) as a white solid. $MS(ES)^+$ m/e 479.2 $[M+H]^+$. $^1H$ NMR (400 MHz, DMSO-$d_6$) $\delta$ ppm 9.89 (s, 1H), 7.68 (s, 1H), 7.48 - 7.60 (m, 1H), 7.09 - 7.36 (m, 5H), 6.90 (d, *J* = 7.58 Hz, 1H), 5.42 (d, *J* = 12.13 Hz, 2H), 4.79 - 5.15 (m, 1H), 4.08 - 4.30 (m, 1H), 3.79 - 3.99 (m, 1H), 2.93 - 3.24 (m, 2H), 2.30 (s, 3H), 1.43 (br. s., 9H), 1.02 (br. s., 3H).

**Step e) 1-(4-fluorobenzyl)-7-methyl-*N*-(*m*-tolyl)-4,5,6,7-tetrahydro-1*H*-pyrazolo[4,3-*c*]pyridine-3-carboxamide hydrochloride (15)**

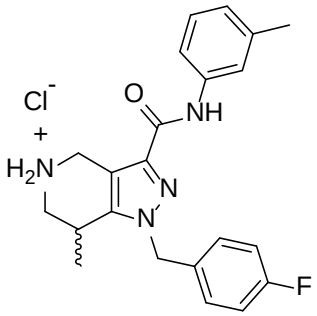


To round-bottom flask containing *tert*-butyl 1-(4-fluorobenzyl)-7-methyl-3-(*m*-tolylcarbamoyl)-6,7-dihydro-1*H*-pyrazolo[4,3-c]pyridine-5(4*H*)-carboxylate (558mg, 1.17 mmol) was added HCl (4N in 1,4-dioxane, 1458 μL, 5.83 mmol). The resulting clear solution was stirred at room temperature for 2 hours. The reaction mixture was concentrated under reduced pressure and the resulting residue was dried to constant weight under high vacuum to provide 1-(4-fluorobenzyl)-7-methyl-*N*-(*m*-tolyl)-4,5,6,7-tetrahydro-1*H*-pyrazolo[4,3-*c*]pyridine-3-carboxamide hydrochloride (495 mg, 1.193 mmol, quantitative yield) as a white solid. This material was used without further purification. MS(ES)$^+$ m/e 379.5 $[M+H]^+$. $^1$H NMR (400 MHz, DMSO-$d_6$) δ ppm 10.08 (s, 1H), 9.54 (br. s., 1H), 9.04 (br. s., 1H), 7.67 (s, 1H), 7.57 (d, *J* = 8.84 Hz, 1H), 7.12 - 7.37 (m, 5H), 6.92 (d, *J* = 7.58 Hz, 1H), 5.35 - 5.59 (m, 2H), 4.32 (br. s., 2H), 3.22 - 3.33 (m, 3H), 2.26 - 2.32 (m, 3H), 1.25 (d, *J* = 6.82 Hz, 3H).

**Step f) (7*R*)-1-[(4-fluorophenyl)methyl]-7-methyl-*N*-(3-methylphenyl)-5-(1*H*-pyrrol-2-ylcarbonyl)-4,5,6,7-tetrahydro-1*H*-pyrazolo[4,3-*c*]pyridine-3-carboxamide (GSK303)**

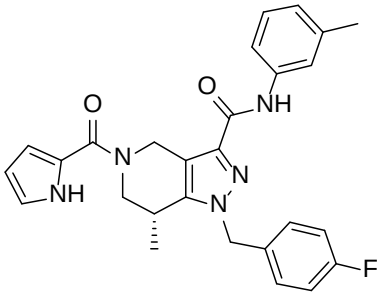


To a solution of 1-(4-fluorobenzyl)-7-methyl-*N*-(*m*-tolyl)-4,5,6,7-tetrahydro-1*H*-pyrazolo[4,3-*c*]pyridine-3-carboxamide hydrochloride (0.200 g, 0.48 mmol) in DCM (5 mL) were added 1*H*-pyrrole-2-carboxylic acid (0.060 mL, 0.53 mmol), HATU (0.275 g, 0.72 mmol) and i-$Pr_2$NEt (0.253 mL, 1.45 mmol). The mixture was stirred at room temperature under nitrogen 16 hours, quenched with water and the aqueous layer was extracted with two portions of DCM. The combined DCM extracts were dried over $Na_2SO_4$, filtered and concentrated under reduced pressure. The residue was purified by silica gel chromatography (Analogix, SF25-40 g column, 50-60 % EtOAc in hexanes). The appropriate fractions were combined and concentrated under reduced pressure. The solid residue was triturated with 20 % EtOAc/hexanes, collected by filtration and

dried to constant weight under high vacuum to provide racemic 1-[(4-fluorophenyl)methyl]-7-methyl-*N*-(3-methylphenyl)-5-(1*H*-pyrrol-2-ylcarbonyl)-4,5,6,7-tetrahydro-1*H*-pyrazolo[4,3-*c*]pyridine-3-carboxamide (0.170 g, 0.361 mmol, 74 % yield) as a white solid. This material was purified by chiral prep HPLC (Chiralpak IA 21 x 250 mm; $CH_3CN$:$CH_3OH$- 95:5; 20 ml/min; uv 250 nm) to provide:

Rt 6.0 min: (7*R*)-1-[(4-fluorophenyl)methyl]-7-methyl-*N*-(3-methylphenyl)-5-(1*H*-pyrrol-2-ylcarbonyl)-4,5,6,7-tetrahydro-1*H*-pyrazolo[4,3-*c*]pyridine-3-carboxamide as a white solid. $^1$H NMR (400 MHz, DMSO-$d_6$) $\delta$ 11.56 (br. s., 1H), 9.91 (s, 1H), 7.69 (s, 1H), 7.56 (d, *J* = 8.08 Hz, 1H), 7.24 - 7.31 (m, 2H), 7.15 - 7.24 (m, 3H), 6.85 - 6.96 (m, 2H), 6.59 (br. s., 1H), 6.11 - 6.24 (m, 1H), 5.38 - 5.53 (m, 2H), 5.31 (d, *J* = 16.42 Hz, 1H), 4.68 (br. s., 1H), 4.35 (d, *J* = 11.12 Hz, 1H), 3.36 - 3.45 (m, 1H), 3.09 - 3.22 (m, 1H), 2.30 (s, 3H), 1.09 (d, 3H). $^{13}$C NMR spectra generally complex for this series due to presence of rotamers and $^{19}$F splitting. $^{13}$C NMR (100.61 MHz, DMSO-$d_6$) 163.24, 162.94, 160.89, 160.83, 144.20, 141.06, 138.93, 138.16, 133.56, 129.93, 129.56, 129.37, 129.30, 128.96, 128.68, 124.85, 121.48, 121.24, 118.00, 116.22, 116.01, 115.58, 112.49, 112.25, 109.07, 108.98, 52.17, 27.83, 21.70, 21.64, 18.61. MS(ES)$^+$ m/e 472.3 $[M+H]^+$. $[\alpha]_D$ = + 155° (c = 0.1 , $CH_3CN$:$CH_3OH$- 95:5). The absolute stereochemistry was determined by VCD analysis.

The opposite enantiomer was also isolated, Rt 9.9 min: (7*S*)-1-[(4-fluorophenyl)methyl]-7-methyl-*N*-(3-methylphenyl)-5-(1*H*-pyrrol-2-ylcarbonyl)-4,5,6,7-tetrahydro-1*H*-pyrazolo[4,3-*c*]pyridine-3-carboxamide as a white solid . $^1$H NMR (400 MHz, DMSO-$d_6$) $\delta$ ppm 11.56 (br. s., 1H), 9.91 (s, 1H), 7.69 (s, 1H), 7.56 (d, *J* = 8.08 Hz, 1H), 7.24 - 7.32 (m, 2H), 7.13 - 7.24 (m, 3H), 6.84 - 6.96 (m, 2H), 6.59 (br. s., 1H), 6.14 - 6.23 (m, 1H), 5.37 - 5.55 (m, 2H), 5.31 (d, *J* = 16.42 Hz, 1H), 4.67 (br. s., 1H), 4.36 (d, *J* = 13.14 Hz, 1H), 3.37 - 3.49 (m, 1H), 3.11 - 3.23 (m, 1H), 2.30 (s, 3H), 1.09 (d, 3H). MS(ES)$^+$ m/e 472.2 $[M+H]^+$. $[\alpha]_D$ = -140 ° (c = 0.03, $CH_3CN$:$CH_3OH$- 95:5). The absolute stereochemistry was determined by VCD analysis.

**(7*R*)-1-[(4-fluorophenyl)methyl]-*N*-{3-[(1*S*)-1-hydroxyethyl]phenyl}-7-methyl-5-(1*H*-pyrrol-2-ylcarbonyl)-4,5,6,7-tetrahydro-1*H*-pyrazolo[4,3-*c*]pyridine-3-carboxamide (GSK321)**

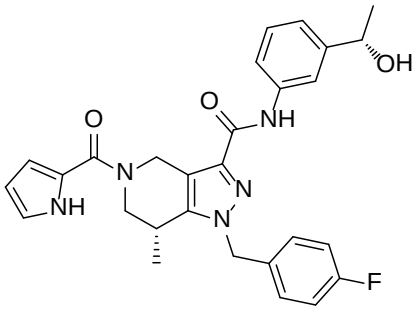


**Step d) *tert*-butyl 1-(4-fluorobenzyl)-3-((3-(1-hydroxyethyl)phenyl)carbamoyl)-7-methyl-6,7-dihydro-1*H*-pyrazolo[4,3-c]pyridine-5(4*H*)-carboxylate (16)**

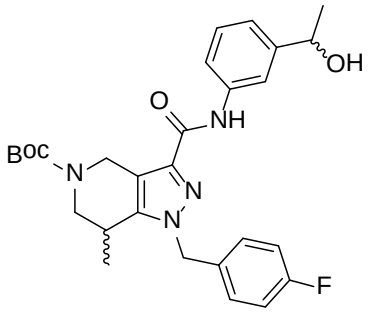


To a mixture of 5-(*tert*-butoxycarbonyl)-1-(4-fluorobenzyl)-7-methyl-4,5,6,7-tetrahydro-1*H*-pyrazolo[4,3-*c*]pyridine-3-carboxylic acid (240 mg, 0.62 mmol), 1-(3-aminophenyl)ethanol (127 mg, 0.92 mmol), HOBT (142 mg, 0.92 mmol) and EDC (177 mg, 0.92 mmol) were added THF (9 mL) and i-$Pr_2$NEt (0.323 mL, 1.85 mmol) and the reaction mixture was stirred for 4 h at 35 °C. The reaction mixture was concentrated under reduced pressure and the residue was dissolved in DCM, washed with water, dried over sodium sulfate, filtered and evaporated to provide *tert*-butyl 1-(4-fluorobenzyl)-3-((3-(1-hydroxyethyl)phenyl)carbamoyl)-7-methyl-6,7-dihydro-1*H*-pyrazolo[4,3-c]pyridine-5(4*H*)-carboxylate (310 mg, 0.61 mmol, 99 % yield). MS(ES)$^+$ m/e 509.1 $[M+H]^+$.

**Steps e & f) (7*R*)-1-[(4-fluorophenyl)methyl]-*N*-{3-[(1*S*)-1-hydroxyethyl]phenyl}-7-methyl-5-(1*H*-pyrrol-2-ylcarbonyl)-4,5,6,7-tetrahydro-1*H*-pyrazolo[4,3-*c*]pyridine-3-carboxamide (GSK321)**

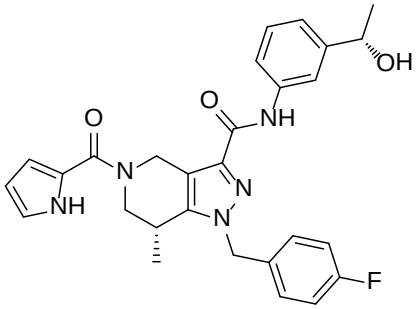


To *tert*-butyl 1-(4-fluorobenzyl)-3-((3-(1-hydroxyethyl)phenyl)carbamoyl)-7-methyl-6,7-dihydro-1*H*-pyrazolo[4,3-c]pyridine-5(4*H*)-carboxylate (310 mg, 0.61 mmol) in a flask was added 4N HCl in 1,4-dioxane (1.5 mL). The reaction mixture was stirred for 2 h at room temperature. The solvent was removed under reduced pressure and the residue was azeotroped with THF and dissolved in THF (9 mL). To this mixture were added 1*H*-pyrrole-2-carboxylic acid (103 mg, 0.92 mmol), HOBT (142 mg, 0.92 mmol), EDC (177 mg, 0.92 mmol) and i-$Pr_2$NEt (0.323 ml, 1.85 mmol). The reaction mixture was stirred for 18 h at 25 °C. The reaction mixture was concentrated under reduced pressure and the residue was dissolved in EtOAc and washed with water. The solution was dried over sodium sulfate, filtered and evaporated under vacuum to give 350 mg of crude product which was purified on silica gel (13 – 100 % EtOAc in hexanes). The combined fractions provided 174 mg of product. This material was further purified on

silica gel (0 – 1 % DCM in MeOH) to provide a four component stereoisomeric mixture containing the titled compound (124 mg, 0.242 mmol, 39 % yield). MS(ES)$^+$ m/e 502.1 $[M+H]^+$.

The four stereoisomers were separated by chiral preparative HPLC using the following method: 1-[(4-Fluorophenyl)methyl]-*N*-{3-[1-hydroxyethyl]phenyl}-7-methyl-5-(1*H*-pyrrol-2-ylcarbonyl)-4,5,6,7-tetrahydro-1*H*-pyrazolo[4,3-*c*]pyridine-3-carboxamide (88 mg) was dissolved in ethanol and applied to a column (Chromegachiral CC4, 30 x 250 mm, 5u). Elution with heptane:ethanol (60:40) at 45 mL/min and UV detection of 254 nm provided complete separation of two stereoisomers, E1 and E2, with elution times of 9.5 and 24.6 min respectively and a fraction containing a mixture of two different stereoisomers. (7*R*)-1-[(4-fluorophenyl)methyl]-*N*-{3-[(1*S*)-1-hydroxyethyl]phenyl}-7-methyl-5-(1*H*-pyrrol-2-ylcarbonyl)-4,5,6,7-tetrahydro-1*H*-pyrazolo[4,3-*c*]pyridine-3-carboxamide was obtained as E1 from the above chiral prep HPLC (18.6 mg, 0.037 mmol). MS(ES)$^+$ m/e 502.3 $[M+H]^+$. $[\alpha]_D$ +110° (c = 0.02, 1:1 heptane:EtOH). $^1$H NMR (400 MHz, DMSO-$d_6$) $\delta$ ppm 11.55 (br. s., 1 H), 9.91 (s, 1 H), 7.83 (s, 1 H), 7.62 - 7.64 (m, 1 H), 7.18 - 7.30 (m, 5 H), 7.06 (d, *J* = 7.83 Hz, 1 H), 6.92 (br. s., 1 H), 6.5 - 6.6 (m, 1 H), 6.17 - 6.19 (m, 1 H), 5.43 - 5.55 (q, 2 H), 5.29 (m, 1 H), 4.58 - 4.78 (m, 2 H), 4.35 (d, *J* = 11.62 Hz, 1 H), 3.36 - 3.48 (m, 2 H), 3.05 - 3.23 (m, 1 H), 1.33 (d, *J* = 6.32 Hz 3 H), 1.09 (d, *J* = 6.82 Hz, 3 H). $^{13}$C NMR spectra generally complex for this series due to presence of rotamers and $^{19}$F splitting. The absolute stereochemistry was determined by VCD analysis.

**Synthesis of GSK864 (4)** [a]

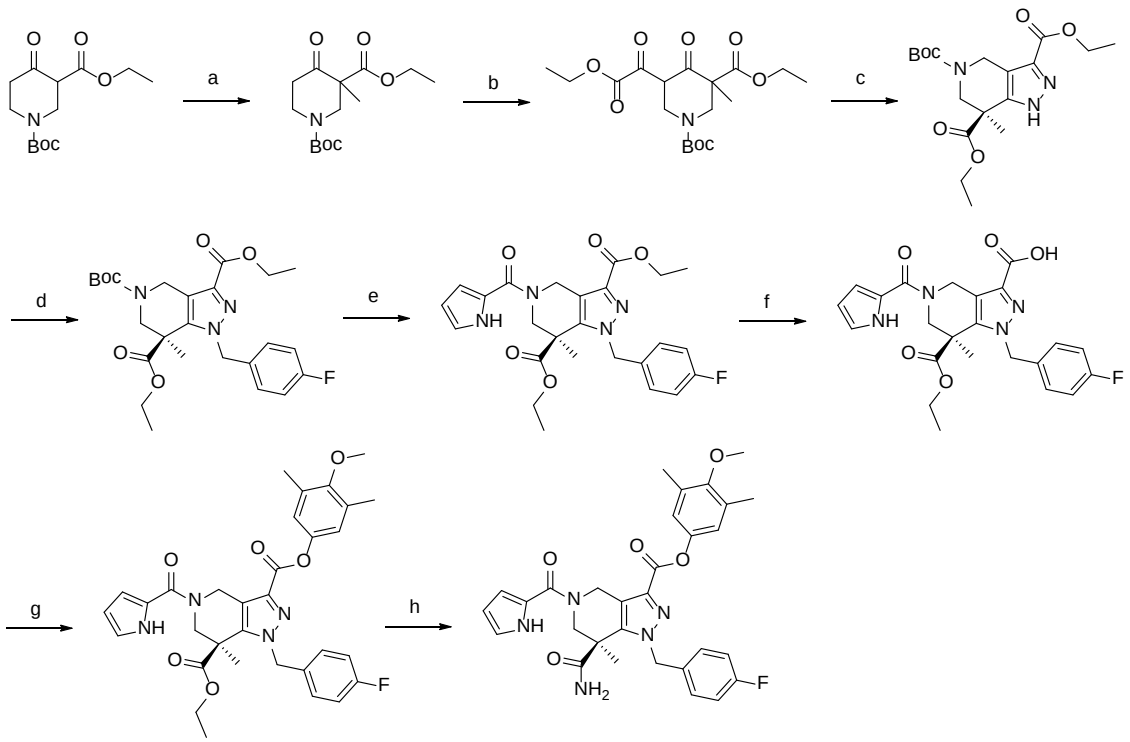

[a]Reagents and Conditions: (a) NaH, MeI, DMF, 0 °C to rt; (b) LDA, THF, 0 °C to rt, then diethyl oxalate, 0 °C to rt; (c) hydrazine hydrate, DCM; then chiral prep HPLC; (d) NaH, 1-(bromomethyl)-4-fluorobenzene, EtOAc; (e) 4M HCl in 1,4-dioxane, $CHCl_3$, 50 °C; then 1*H*-pyrrole-2-carboxylic acid, EDC, HOBt, TEA, DMSO, 55 °C; (f) NaOH, EtOH, water; (g) 4-methoxy-3,5-dimethylaniline, COMU, 4-methylmorpholine, EtOAc; (h) NaOH, EtOH, water; then $NH_3$ in 1,4-dioxane, HATU, EDC, TEA, 40 °C.

**_(S)_-1-(4-fluorobenzyl)-N3-(4-methoxy-3,5-dimethylphenyl)-7-methyl-5-(1*H*-pyrrole-2-carbonyl)-4,5,6,7-tetrahydro-1*H*-pyrazolo[4,3-c]pyridine-3,7-dicarboxamide (GSK864)**

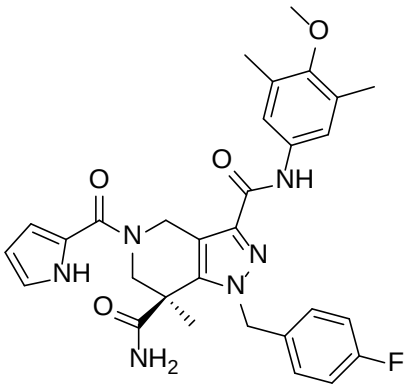

**Step a) 1-*tert*-butyl 3-ethyl 3-methyl-4-oxopiperidine-1,3-dicarboxylate (17)**

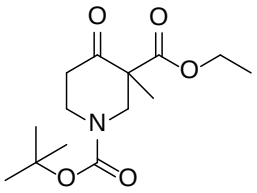

A solution of 1-*tert*-butyl 3-ethyl 4-hydroxy-5,6-dihydropyridine-1,3(2*H*)-dicarboxylate (50 g, 184 mmol) in DMF (100 mL) was added dropwise to a cooled suspension (0 °C) of 60 % sodium hydride in mineral oil (8.0 g, 200 mmol) in DMF (100 mL). The cooling bath was removed and the mixture was stirred until all NaH had dispersed, about 1 hr. The mixture was treated with iodomethane (13.77 mL, 221 mmol) in DMF (50 mL) and the mixture was stirred for 2 hours. The mixture was partitioned between ethyl acetate and 1 M hydrochloric acid. The layers were separated and the aqueous was extracted with ethyl acetate (x2). The combined extracts were washed with 1M hydrochloric acid and brine, dried ($Na_2SO_4$) and evaporated. Silica gel chromatography (120 g column + 20 g header, 10-50 % ethyl acetate in hexane) gave 1-tert-butyl 3-ethyl 3-methyl-4-oxopiperidine-1,3-dicarboxylate (45.7 g, 160 mmol, 87 % yield). MS(ES)$^+$ m/e 286.0 $[M+H]^+$. $^1$H NMR (400 MHz, CHLOROFORM-*d*) $\delta$ ppm 1.28 (t, *J* = 7.07 Hz, 3 H), 1.32 (s, 3 H), 1.50 (s, 9 H), 2.50 (dt, *J* = 14.72, 4.01 Hz, 1 H), 2.78 (br. s., 1 H), 3.07 (d, *J* = 13.64 Hz, 1 H), 3.25 - 3.43 (m, 1 H), 3.93 - 4.32 (m, 3 H), 4.54 (d, *J* = 11.87 Hz, 1 H).

**Step b) 1-*tert*-butyl 3-ethyl 5-(2-ethoxy-2-oxoacetyl)-3-methyl-4-oxopiperidine-1,3-dicarboxylate (18)**

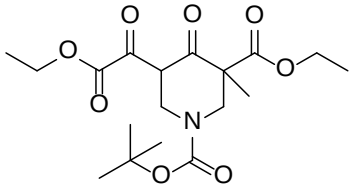

A solution of LDA was prepared by adding n-butyllithium (785 mL, 1256 mmol) to a precooled solution (at 0 °C using an ice water bath) of diisopropylamine (215 mL, 1507 mmol) in tetrahydrofuran (1 L). The solution was stirred at 0 °C for 45 min. To the LDA solution was added a solution of 1-*tert*-butyl 3-ethyl 3-methyl-4-oxopiperidine-1,3-dicarboxylate (358.4 g, 1256 mmol) in tetrahydrofuran (1.5 L) dropwise over 30 minutes while maintaining the temperature at 0 °C. The cooling bath was removed and the mixture was stirred for 45 minutes at room temperature. The mixture was re-cooled to 0 °C and a solution of diethyl oxalate (275 g, 1884 mmol) in THF (0.5 L) was added dropwise over 15 minutes. The mixture was allowed to warm to ambient temperature, stirred for 3 hours, quenched with sat. ammonium chloride solution and diluted with ethyl acetate. The aqueous layer was extracted with ethyl acetate and the combined organic extracts were washed with 1M hydrochloric acid. The aqueous layer was back-extracted with ethyl acetate and the combined extracts washed with brine, dried ($Na_2SO_4$), filtered and evaporated to give 1-*tert*-butyl 3-ethyl 5-(2-ethoxy-2-oxoacetyl)-3-methyl-4-oxopiperidine-1,3-dicarboxylate (475.5 g, 1234 mmol, 98 % yield) as a thick yellow oil. MS(ES)$^+$ m/e 386.2 $[M+H]^+$.

**Step c) *(S)*-5-*tert*-butyl 3,7-diethyl 7-methyl-6,7-dihydro-1*H*-pyrazolo[4,3-*c*]pyridine-3,5,7(4*H*)-tricarboxylate (19)**

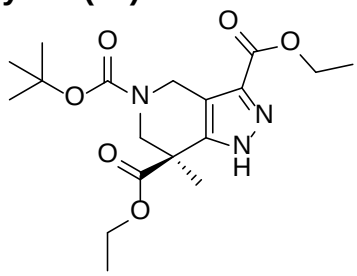

A solution of 1-*tert*-butyl 3-ethyl 5-(2-ethoxy-2-oxoacetyl)-3-methyl-4-oxopiperidine-1,3-dicarboxylate (435 g, 1129 mmol) in dichloromethane (2 L) was treated with hydrazine hydrate (0.082 L, 1693 mmol) and stirred for 2 hrs. The solvent was evaporated and the crude residue was purified on silica gel (dichloromethane to 5 % methanol in dichloromethane) to give 5-*tert*-butyl 3,7-diethyl 7-methyl-6,7-dihydro-1*H*-pyrazolo[4,3-*c*]pyridine-3,5,7(4*H*)-tricarboxylate (237.8 g, 623 mmol, 55 % yield). LCMS m/e 382.2 $[M+H]^+$. The enantiomers were separated using Prep chiral SFC (Chiralpak AD-H 5u 30 x 250 mm; eluting with 30 % $CH_3OH$ @ 70 ml/min; 30 deg C 100 bar o.p. uv 254 nm) to give E1 (97.1 g) as a glassy solid; chiral SFC > 99 % ee; LCMS m/e 382 $[M+H]^+$; Alpha D = - 65 deg (c = 0.3, $CH_3OH$) and E2, 92.9 g as a glassy solid; chiral SFC 96 % ee; $MS(ES)^+$ m/e 382 $[M+H]^+$; $[\alpha]_D$ +67° (c = 0.3, $CH_3OH$). The (-)-enantiomer was determined to have the *(S)*-configuration by VCD analysis, thereby providing *(S)*-5-*tert*-butyl 3,7-diethyl 7-methyl-6,7-dihydro-1*H*-pyrazolo[4,3-*c*]pyridine-3,5,7(4*H*)-tricarboxylate.

**Step d) *(S)*-5-*tert*-butyl 3,7-diethyl 1-(4-fluorobenzyl)-7-methyl-6,7-dihydro-1*H*-pyrazolo[4,3-*c*]pyridine-3,5,7(4*H*)-tricarboxylate (20)**

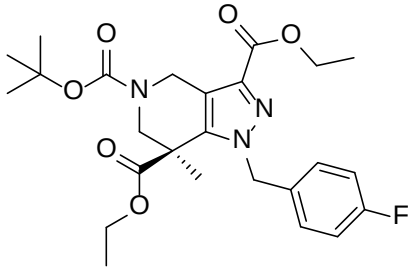

A solution of (-)-*(S)*-5-*tert*-butyl 3,7-diethyl 7-methyl-6,7-dihydro-1*H*-pyrazolo[4,3-*c*]pyridine-3,5,7(4*H*)-tricarboxylate (25.4 g, 66.6 mmol) in ethyl acetate (500 mL) under $N_2$ was treated with sodium hydride (3.20 g, 80 mmol) and the mixture was stirred for 1 hour. 1-(Bromomethyl)-4-fluorobenzene (7.18 mL, 69.9 mmol) was added and the mixture was stirred over the weekend. The mixture was diluted with ethyl acetate and washed with 1M HCl. The aqueous layer was extracted with ethyl acetate (x2) and the combined extracts were washed with brine, concentrated onto silica gel and purified by silica gel chromatography (150 g, hexane - 30% ethyl acetate in hexane) to give *(S)*-5-

*tert*-butyl 3,7-diethyl 1-(4-fluorobenzyl)-7-methyl-6,7-dihydro-1*H*-pyrazolo[4,3-*c*]pyridine-3,5,7(4*H*)-tricarboxylate (23.9 g, 47.8 mmol, 71% yield) as an oil. $MS(ES)^+$ m/e 490.2 $[M+H]^+$. $^1H$ NMR (400 MHz, DICHLOROMETHANE-$d_2$) $\delta$ ppm 1.16 (t, *J* = 7.20 Hz, 3 H), 1.36 - 1.45 (m, 6 H), 1.48 (s, 9 H), 3.43 - 4.24 (m, 4 H), 4.39 (q, *J* = 7.07 Hz, 2 H), 4.48 - 4.93 (m, 2 H), 5.17 - 5.34 (m, 2 H), 6.97 - 7.18 (m, 4 H).

**Step e) *(S)*-diethyl 1-(4-fluorobenzyl)-7-methyl-5-(1*H*-pyrrole-2-carbonyl)-4,5,6,7-tetrahydro-1*H*-pyrazolo[4,3-c]pyridine-3,7-dicarboxylate (21)**

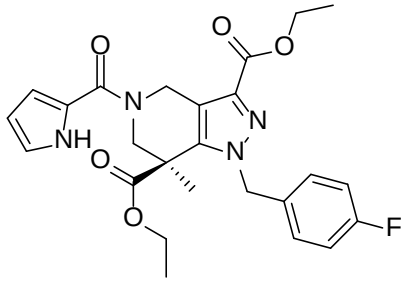


A solution of *(S)*-5-*tert*-butyl 3,7-diethyl 1-(4-fluorobenzyl)-7-methyl-6,7-dihydro-1*H*-pyrazolo[4,3-*c*]pyridine-3,5,7(4*H*)-tricarboxylate (23.9 g, 48.8 mmol) in chloroform (50 mL) was treated with 4M hydrogen chloride in 1,4-dioxane (50 mL, 200 mmol) and stirred at 50 °C for 1 hour. The reaction mixture was concentrated under reduced pressure, taken up in DMSO (50 mL) and added to an aged (30 min) mixture of EDC (11.23 g, 58.6 mmol), HOBt (8.97 g, 58.6 mmol), 1*H*-pyrrole-2-carboxylic acid (8.14 g, 73.2 mmol) and triethylamine (20.41 mL, 146 mmol) in dimethyl sulfoxide (100 mL). The mixture was stirred overnight at 55 °C, cooled to room temperature and diluted with ethyl acetate. The organic layer was washed with water and the aqueous layer was back-extracted with ethyl acetate. The combined organics were washed with 1M HCl. The combined aqueous solutions were further extracted with ethyl acetate (x3) and the combined organics were washed with brine and evaporated. Silica gel chromatography (400 g, 20-70% ethyl acetate in hexanes) gave *(S)*-diethyl 1-(4-fluorobenzyl)-7-methyl-5-(1*H*-pyrrole-2-carbonyl)-4,5,6,7-tetrahydro-1*H*-pyrazolo[4,3-*c*]pyridine-3,7-dicarboxylate (17.5 g, 35.9 mmol, 73.5 % yield) as a foam. $MS(ES)^+$ m/e 483.0 $[M+H]^+$. $^1H$ NMR (400 MHz, DICHLOROMETHANE-$d_2$) $\delta$ ppm 1.11 (t, *J* = 7.07 Hz, 3 H), 1.44 (t, *J* = 7.20 Hz, 3 H), 1.48 (s, 3 H), 3.83 (dq, *J* = 10.77, 7.19 Hz, 1 H), 3.96 (d, *J* = 13.14 Hz, 1 H), 4.05 (dq, *J* = 10.83, 7.17 Hz, 1 H), 4.24 (d, *J* = 13.14 Hz, 1 H), 4.41 (q, *J* = 7.07 Hz, 2 H), 5.15 (br. s., 2 H), 5.24 - 5.40 (m, 2 H), 6.29 - 6.37 (m, 1 H), 6.72 - 6.80 (m, 1 H), 6.99 (td, *J* = 2.65, 1.26 Hz, 1 H), 7.02 - 7.16 (m, 4 H), 9.67 (br. s., 1 H).

**Step f) *(S)*-7-(ethoxycarbonyl)-1-(4-fluorobenzyl)-7-methyl-5-(1*H*-pyrrole-2-carbonyl)-4,5,6,7-tetrahydro-1*H*-pyrazolo[4,3-c]pyridine-3-carboxylic acid (22)**

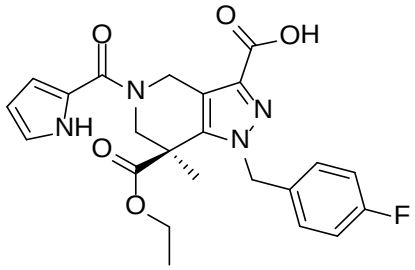

A solution of *(S)*-diethyl 1-(4-fluorobenzyl)-7-methyl-5-(1*H*-pyrrole-2-carbonyl)-4,5,6,7-tetrahydro-1*H*-pyrazolo[4,3-*c*]pyridine-3,7-dicarboxylate (24 g, 49.7 mmol) in ethanol (400 mL) was treated with 1.0M NaOH solution (59.7 mL, 59.7 mmol) and stirred for 2 hours. The mixture was diluted with 1M HCl (1000 mL) and partitioned with ethyl acetate. The aqueous phase was extracted with ethyl acetate (x3) and the combined extracts were dried over $MgSO_4$, filtered and evaporated to give *(S)*-7-(ethoxycarbonyl)-1-(4-fluorobenzyl)-7-methyl-5-(1*H*-pyrrole-2-carbonyl)-4,5,6,7-tetrahydro-1*H*-pyrazolo[4,3-c]pyridine-3-carboxylic acid (22 g, 38.7 mmol, 78 % yield) as a foam. MS(ES)$^+$ m/e 455.1 $[M+H]^+$. $^1$H NMR (400 MHz, CHLOROFORM-*d*) $\delta$ ppm 1.12 (t, 3 H), 1.48 (s, 3 H), 3.76 - 3.91 (m, 1 H), 3.99 - 4.10 (m, 2 H), 4.22 (d, *J* = 12.63 Hz, 1 H), 4.39 - 4.56 (m, 1 H), 5.09 - 5.43 (m, 4 H), 6.30 - 6.40 (m, 1 H), 6.79 (br. s., 1 H), 6.96 - 7.05 (m, 3 H), 7.11 (dd, *J* = 8.59, 5.31 Hz, 2 H), 9.83 (br. s., 1 H).

**Step g) *(S)*-ethyl 1-(4-fluorobenzyl)-3-((4-methoxy-3,5-dimethylphenyl)carbamoyl)-7-methyl-5-(1*H*-pyrrole-2-carbonyl)-4,5,6,7-tetrahydro-1*H*-pyrazolo[4,3-c]pyridine-7-carboxylate (23)**

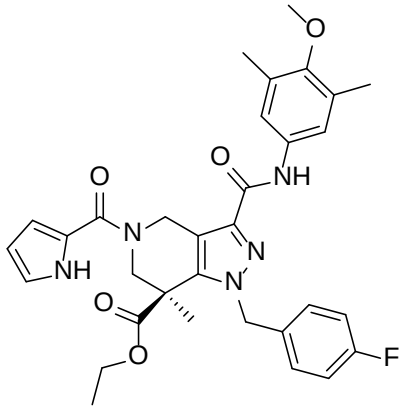

A solution of *(S)*-7-(ethoxycarbonyl)-1-(4-fluorobenzyl)-7-methyl-5-(1*H*-pyrrole-2-carbonyl)-4,5,6,7-tetrahydro-1*H*-pyrazolo[4,3-c]pyridine-3-carboxylic acid (18 g, 39.6 mmol) in ethyl acetate (350 mL) was treated with COMU (20.36 g, 47.5 mmol) and 4-methylmorpholine (5.23 mL, 47.5 mmol). After 15 minute (some warming was required to obtain a solution), 4-methoxy-3,5-dimethylaniline (7.19 g, 47.5 mmol) was added and the mixture was stirred for 1 hour at room temperature. The reaction mixture was washed with water, 1M HCl and brine. The organic layer was concentrated under reduced pressure and the residue was purified by silica gel chromatography (20-50 % EtOAc in hexanes) to give *(S)*-ethyl 1-(4-fluorobenzyl)-3-((4-methoxy-3,5-dimethylphenyl)carbamoyl)-7-methyl-5-(1*H*-pyrrole-2-carbonyl)-4,5,6,7-tetrahydro-1*H*-

pyrazolo[4,3-c]pyridine-7-carboxylate (12.7 g, 18.37 mmol, 46.4 % yield). MS(ES)$^+$ m/e 588.1 [M+H]$^+$. $^1$H NMR (400 MHz, CHLOROFORM-*d*) δ ppm 1.14 (t, *J* = 7.07 Hz, 3 H), 1.50 (s, 3 H), 2.32 (s, 6 H), 3.73 (s, 3 H), 3.79 - 3.91 (m, 1 H), 3.99 - 4.12 (m, 2 H), 5.08 - 5.46 (m, 4 H), 6.28 - 6.35 (m, 1 H), 6.88 (br. s., 1 H), 6.92 - 6.98 (m, 1 H), 6.99 - 7.17 (m, 5 H), 7.31 (s, 2 H), 8.47 (s, 1 H), 9.37 (br. s., 1 H).

**Step h) *(S)*-1-(4-fluorobenzyl)-N3-(4-methoxy-3,5-dimethylphenyl)-7-methyl-5-(1*H*-pyrrole-2-carbonyl)-4,5,6,7-tetrahydro-1*H*-pyrazolo[4,3-c]pyridine-3,7-dicarboxamide (GSK864)**

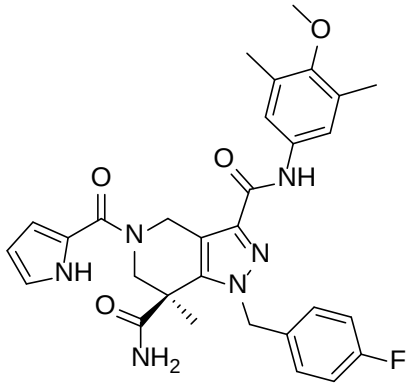


A solution of *(S)*-ethyl 1-(4-fluorobenzyl)-3-((4-methoxy-3,5-dimethylphenyl)carbamoyl)-7-methyl-5-(1*H*-pyrrole-2-carbonyl)-4,5,6,7-tetrahydro-1*H*-pyrazolo[4,3-*c*]pyridine-7-carboxylate (12.7 g, 21.61 mmol) in ethanol (100 mL) was treated with 1.0M sodium hydroxide solution (60 mL, 60.0 mmol) and the mixture was stirred overnight. The mixture was diluted with water and the aqueous layer was washed with diethyl ether, acidified with 1M HCl and extracted with ethyl acetate (x3). The combined extracts were dried ($MgSO_4$) and evaporated to a foam. The residue was treated with HATU (12.33 g, 32.4 mmol), EDC (8.29 g, 43.2 mmol) and triethylamine (9.04 mL, 64.8 mmol). The flask was sealed with a septum, treated with 0.5M ammonia in 1,4-dioxane (216 mL, 108 mmol) and stirred at 40 °C for 1 hour. The mixture was concentrated under reduced pressure. The residue was taken up in ethyl acetate, washed successively with 1M NaOH, 1M HCl and brine. The organic layer was evaporated onto silica gel and purified by silica gel chromatography (120 g column; dichloromethane, then 2 % methanol in dichloromethane, then 5 % methanol in dichloromethane). The desired fractions were concentrated under reduced pressure and the residue was evaporated from ethyl acetate to give *(S)*-1-(4-fluorobenzyl)-N3-(4-methoxy-3,5-dimethylphenyl)-7-methyl-5-(1*H*-pyrrole-2-carbonyl)-4,5,6,7-tetrahydro-1*H*-pyrazolo[4,3-*c*]pyridine-3,7-dicarboxamide (6.9 g, 12.29 mmol, 56 % yield). MS(ES)$^+$ m/e 559.1 [M+H]$^+$. $[\alpha]_D$ -74° (c = 0.50, methanol, 22 °C). $^1$H NMR (400 MHz, DMSO-$d_6$) δ ppm 1.28 (s, 3 H), 2.20 (s, 6 H), 3.62 (s, 3 H), 4.00 (br. s., 2 H), 4.93 (d, *J* = 16.17 Hz, 1 H), 5.15 (d, *J* = 16.93 Hz, 1 H), 5.25 - 5.48 (m, 2 H), 6.14 - 6.24 (m, 1 H), 6.64 (br. s., 1 H), 6.89 - 6.99 (m, 1 H), 7.09 - 7.31 (m, 4 H), 7.45 (s, 3 H), 7.54 (br. s., 1 H), 9.76 (s, 1 H), 11.60 (br. s., 1 H). $^{13}$C NMR spectra generally complex for this series due to presence of rotamers and $^{19}$F splitting. $^{13}$C NMR (100.61 MHz, $CDCl_3$) 175.22, 163.43,

163.15, 160.98, 159.85, 153.67, 141.41, 140.51, 133.05, 132.85, 131.50, 128.57, 128.37, 123.13, 122.83, 122.40, 120.66, 120.41, 116.06, 115.61, 110.54, 59.92, 59.74, 54.80, 50.13, 45.22, 45.04, 23.32, 23.19, 16.22, 16.17 (rotamers and and $^{19}F$ splitting present). Anal. calcd for $C_{30}H_{31}FN_6O_4$-0.1 $H_2O$-0.16 EtOAc: C, 64.00; H, 5.65; N, 14.62. Found C, 63.57; H, 5.66; N, 14.46.

**Synthesis of GSK990 (2)** [a]

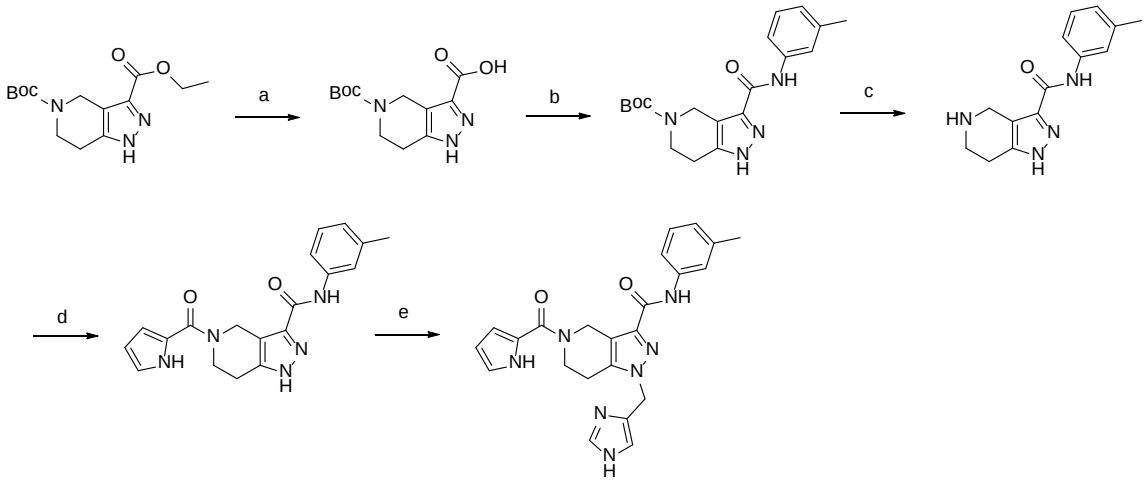


[a]Reagents and Conditions: (a) NaOH, EtOH, water; (b) m-toluidine, HATU, i-$Pr_2$NEt, DMF; (c) TFA, DCM, then aqueous $NaHCO_3$; (d) 1*H*-pyrrole-2-carboxylic acid, HATU, i-$Pr_2$NEt, DCM; (e) 4-(chloromethyl)-1*H*-imidazole-hydrochloride, $Cs_2CO_3$, DMF, 60 °C.

**1-((1*H*-imidazol-4-yl)methyl)-5-(1*H*-pyrrole-2-carbonyl)-*N*-(*m*-tolyl)-4,5,6,7-tetrahydro-1*H*-pyrazolo[4,3-*c*]pyridine-3-carboxamide (GSK990)**

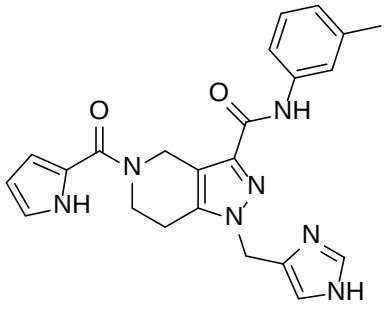

**Step a) 5-(*tert*-butoxycarbonyl)-4,5,6,7-tetrahydro-1*H*-pyrazolo[4,3-*c*]pyridine-3-carboxylic acid (24)**

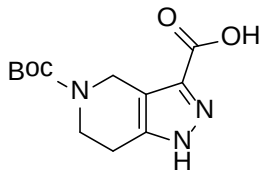


To a solution of 5-*tert*-butyl 3-ethyl 6,7-dihydro-1*H*-pyrazolo[4,3-*c*]pyridine-3,5(4*H*)-dicarboxylate (15 g, 50.8 mmol) in EtOH (300 mL) was added 4 N NaOH (50 mL, 200 mmol). The reaction mixture was stirred at room temperature for 6 hours and concentrated under reduced pressure. The residue was dissolved in water and the pH was adjusted to 5 with 1 N HCl. The resulting precipitate was collected by filtration to provide 5-(*tert*-butoxycarbonyl)-4,5,6,7-tetrahydro-1*H*-pyrazolo[4,3-*c*]pyridine-3-carboxylic acid (11.76 g, 44.0 mmol, 86.7% yield) as a white solid. MS(ES)$^+$ m/e 212.1 [M+H-56]$^+$. $^1$H NMR (300 MHz, DMSO-$d_6$) $\delta$ ppm 13.13 (br. s., 1H), 4.48 (s, 2H), 3.58 (t, *J* = 5.7 Hz, 2H), 2.64 (t, *J* = 5.7 Hz, 2H), 1.42 (s, 9H).

**Step b) *tert*-butyl 3-(*m*-tolylcarbamoyl)-6,7-dihydro-1*H*-pyrazolo[4,3-*c*]pyridine-5(4*H*)-carboxylate (25)**

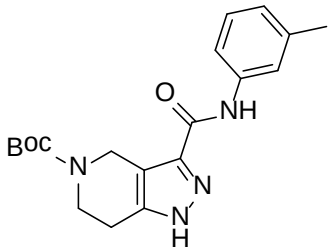


A mixture of 5-(*tert*-butoxycarbonyl)-4,5,6,7-tetrahydro-1*H*-pyrazolo[4,3-*c*]pyridine-3-carboxylic acid (10.7 g, 40 mmol), *m*-toluidine (18 g, 48 mmol), HATU (18 g, 48 mmol) and DIPEA (7.8 g, 60 mmol) was stirred in anhydrous DMF (300 mL) at room temperature overnight. The reaction mixture was poured into water (200 mL) and extracted with EtOAc (150 mL x 3). The combined organic extracts were washed with brine (200 mL x 3), dried over $Na_2SO_4$, filtered and concentrated under reduced pressure. The residue was purified by silica gel chromatography (PE:EA = 1:10) to provide *tert*-butyl 3-(*m*-tolylcarbamoyl)-6,7-dihydro-1*H*-pyrazolo[4,3-*c*]pyridine-5(4*H*)-carboxylate (14 g, 39.33 mmol, 89.7% yield) as a white solid. NMR analysis shows ~0.82 equivalents of DMF that could not be removed. MS(ES)$^+$ m/e 301.1 [M+H-56]$^+$. $^1$H NMR (300 MHz, DMSO-$d_6$) $\delta$ ppm 13.19 (br. s., 1H), 9.86 (s, 1H), 7.70 (s, 1H), 7.57 (d, *J* = 7.8 Hz, 1H), 7.19 (t, *J* = 7.8 Hz, 1H), 6.88 (d, *J* = 7.2 Hz, 1H), 4.56 (s, 2H), 3.62 (t, *J* = 5.7 Hz, 2H), 2.72 (br. s., 2H), 2.29 (s, 3H), 1.43 (s, 9H).

**Step c) *N*-*m*-tolyl-4,5,6,7-tetrahydro-1*H*-pyrazolo[4,3-*c*]pyridine-3-carboxamide (26)**

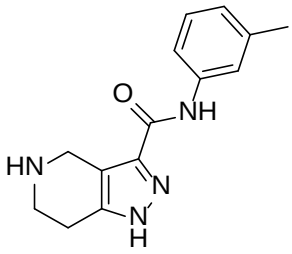

To a solution of *tert*-butyl 3-(*m*-tolylcarbamoyl)-6,7-dihydro-1*H*-pyrazolo[4,3-*c*]pyridine-5(4*H*)-carboxylate (9 g, 25 mmol) in DCM (100 mL) was added TFA (11.5 g, 100 mmol). The reaction mixture was stirred at room temperature for 30 min. The solvent was removed under reduced pressure and the residue was diluted with $NaHCO_3$ (100 mL). The resulting precipitate was collected by filtration and washed with DCM to give *N*-*m*-tolyl-4,5,6,7-tetrahydro-1*H*-pyrazolo[4,3-*c*]pyridine-3-carboxamide (4.0 g, 15.56 mmol, 62% yield) as a light yellow solid. MS(ES)$^+$ m/e 257.2 $[M+H]^+$. $^1$H NMR (300 MHz, DMSO-$d_6$) $\delta$ ppm 13.50 (br. s., 1H), 10.04 (s, 1H), 9.08 (br. s., 1H), 7.68 (s, 1H), 7.57 (d, *J* = 8.1 Hz, 1H), 7.20 (t, *J* = 7.8 Hz, 1H), 6.90 (d, *J* = 7.5 Hz, 1H), 4.35 (s, 2H), 3.42 (t, *J* = 6.0 Hz, 2H), 2.97 (t, *J* = 5.1 Hz, 2H), 2.29 (s, 3H).

**Step d) 5-(1*H*-pyrrole-2-carbonyl)-*N*-*m*-tolyl-4,5,6,7-tetrahydro-1*H*-pyrazolo[4,3-*c*]pyridine-3-carboxamide (27)**

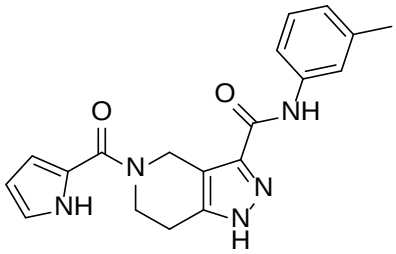

A mixture of *N*-*m*-tolyl-4,5,6,7-tetrahydro-1*H*-pyrazolo[4,3-*c*]pyridine-3-carboxamide (4 g, 16 mmol), 1*H*-pyrrole-2-carboxylic acid (1.91 g, 17 mmol), HATU (8.9 g, 23 mmol) and DIPEA (4 g, 31 mmol) in anhydrous DCM (50 mL) was stirred at room temperature overnight. The reaction mixture was quenched with water (50 mL) and the resulting precipitate was collected by filtration to provide 5-(1*H*-pyrrole-2-carbonyl)-*N*-*m*-tolyl-4,5,6,7-tetrahydro-1*H*-pyrazolo[4,3-*c*]pyridine-3-carboxamide (2.2 g, 6.29 mmol, 40% yield) as a white solid. MS(ES)$^+$ m/e 350.2 $[M+H]^+$. $^1$H NMR (300 MHz, DMSO-$d_6$) $\delta$ ppm 13.23 (s, 1H), 11.52 (br. s., 1H), 9.89 (s, 1H), 7.70 (s, 1H), 7.55 (d, *J* = 8.4 Hz, 1H), 7.17 (t, *J* = 7.8 Hz, 1H), 6.85 - 6.90 (m, 2H), 6.58 (s, 1H), 6.14 - 6.17 (m, 1H), 4.88 - 4.93 (m, 2H), 3.89 - 3.95 (m, 2H), 2.88 - 2.83 (m, 2H), 2.28 (s, 3H).

**Step e) 1-((1*H*-imidazol-4-yl)methyl)-5-(1*H*-pyrrole-2-carbonyl)-*N*-(m-tolyl)-4,5,6,7-tetrahydro-1*H*-pyrazolo[4,3-c]pyridine-3-carboxamide (GSK990)**

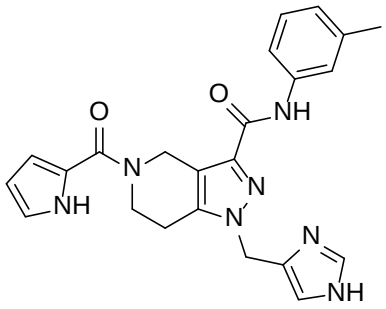


A mixture of 5-(1*H*-pyrrole-2-carbonyl)-*N*-*m*-tolyl-4,5,6,7-tetrahydro-1*H*-pyrazolo[4,3-*c*]pyridine-3-carboxamide (300 mg, 0.87 mmol), 4-(chloromethyl)-1*H*-imidazole-hydrochloride (150 mg, 0.96 mmol) and $Cs_2CO_3$ (1.42 g, 4.35 mmol) in DMF (15 mL) was stirred at 60 °C for 4 hours. The solvent was removed in vacuo and the residue was purified by silica gel chromatography (eluted with 1:100 to 1:30 MeOH:DCM) to provide the title compound. MS(ES)$^+$ m/e 430.1 $[M+H]^+$. $^1$H NMR (400 MHz, DMSO-$d_6$) $\delta$ ppm 12.04 (br. s., 1H), 11.52 (br. s., 1H), 9.82 (s, 1H), 7.70 (s, 1H), 7.60 (s, 1H), 7.55 (d, *J* = 8.34 Hz, 1H), 7.18 (t, *J* = 7.83 Hz, 1H), 7.11 (s, 1H), 6.85-6.94 (m, 2H), 6.57 (br. s., 1H), 6.11-6.22 (m, 1H), 5.26 (s, 2H), 4.91 (br. s., 2H), 3.92 (br. s., 2H), 2.95 (br. s., 2H), 2.29 (s, 3H). $^{13}$C Spectra generally complex for this series due to presence of rotamers.